Transient Effects in Telephone Switching Circuits When Relay Windings are Disconnected

By H. N. WAGAR

(Manuscript received April 1, 1971)

This paper presents an analytical review of the transient events relating to charge, current, voltage, and energy upon disconnection of inductive loads in switching circuits. Based on good agreement between theory and experiment, the analysis is found applicable to a number of long-standing relay and switching circuit problems involving radiation interference, voltage breakdowns in various elements of the contact circuit, and contact erosion.

I. INTRODUCTION

The disconnection of a relay in a switching circuit involves a number of time-variant design problems for which a quantitative treatment is needed. These mainly concern (*i*) the release time of the structure, or (*ii*) the transient current and voltage surges which are a potential cause of oscillations and breakdowns in the circuitry. The subject of release time is chiefly related to a change in the core's magnetization from its operated to its residual value, i.e., a very substantial change in core flux occurring over a comparatively long time, typically several milliseconds. The transient circuit surges tend to develop much earlier in the interval after disconnection, often in times from about 10^{-6} to 10^{-4} second during which the core's magnetization has not yet had time to change appreciably. Thus, while both phenomena are related to the core's demagnetization curve, their performance tends to be controlled by different features of this nonlinear characteristic. The subject of release time, including the design of slow release relays, has been on a firm quantitative basis for many years,[1-4] based on relationships involving the whole demagnetization curve. However, only qualitative or empirical treatments have so far been available to describe the transient surges of current and voltage. An analytical

description of these surges is indispensable to the understanding of voltage breakdowns or radiation interference in the contact wiring; and a renewed interest in these latter subjects has prompted their further study as outlined in this report.

The surges principally result from the tendency for the inductance to maintain current flow after the main current path has been opened; current is then diverted into the circuit capacitances, temporarily charging them to high voltages, even to several hundred times the original battery voltage (when the capacitance is very small). Previous analyses based on a conventional lumped-element L, R, C treatment have not agreed well with experiment, attributed mainly to difficulties in suitably defining the load's nonlinear inductance and to the neglect of eddy current losses in the core. In attempting to recognize these in the present analysis, some simplifications were possible by assuming an effective lumped-element value of inductance which corresponds to the differential permeance of the load's magnetic circuit in the operated region. This concept, and an allowance for eddy current losses, give results which agree well with experiment over several decades of variation in the basic parameters. Over the three decades of principal interest when studying breakdown voltage, this effective inductance is found to be essentially constant, being basically determined by the differential permeance of the core's demagnetization curve at the operated point. Beyond this region, where pulses are slower, the use of a progressively increasing permeance, which recognizes the wider range of the demagnetization curve that comes into play, helps improve the accuracy. The study covered in this report deals mainly with the region where the faster pulses predominate.

1.1 *Outline of Analysis Procedure*

Expressions are first obtained for the general case of a relay winding having both a short-circuited secondary and an RC network, as commonly used for contact protection, bridging the main winding. By assigning suitable values to each of these terms, the results can then be simplified to cover a range of practical situations such as the ordinary unprotected relay coil, the coil bridged by either capacitor or resistor alone, and the air core coil. Of these, the most common case, that of a relay coil shunted only by a capacitor (representing distributed capacitance, wiring capacitance, etc.), is selected for detailed study. Based on good experimental agreement for a wide range of test cases, the results are then applied to a number of special relay and switching circuit design problems.

The surges to be studied are illustrated by the curves in Fig. 1. This view shows a typical relay switching circuit in schematic form, and the transient current and voltage surges when contact X is opened. A major objective is to describe these surges analytically. The initial phase of the analysis is to derive expressions for current and voltage, as a function of time, when the load is disconnected by an "ideal" (i.e., nonbreakdown) contact. The smooth curves in Fig. 1 show typical results when a telephone relay is controlled by a (nonarcing) mercury contact. They have practical interest whenever the switching is done by a vacuum tube, a transistor, or a mercury contact which is well enough insulated to avoid breakdowns. Such curves also determine the conditions for breakdown when apparatus, wiring, or contacts of known dielectric strength are connected in the circuit. For example, the irregular curves in Fig. 1 show the multiple breakdowns that occur across a typical relay contact in air, as its surfaces separate. This result was obtained by replacing the previous mercury contact by an ordinary mechanical contact (on a wire-spring relay) and repeating the measurement as a double exposure on the same film. Such breakdowns, sometimes termed "B-type transients" or "showering arcs," represent successive charging of local capacitance to the dielectric breakdown of the contact's gap, its discharge through the local contact circuit, and a renewed charging cycle. They have been described qualitatively in considerable detail,[5-8] and there have also been some efforts at a quantitative treatment.[9,10] Each successive charging cycle is the beginning of a new "ideal" contact surge; hence the definition of this curve facilitates the study of such breakdowns.

A second phase of the analysis examines these surges from the stand-
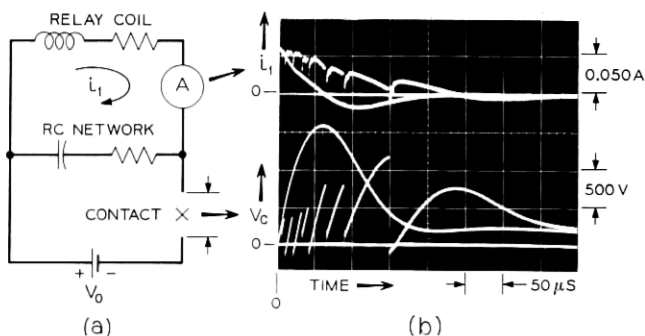

Fig. 1—Surges when contacts open an inductive load. (a) Test Circuit. (b) Current and voltage vs time after interruption for ideal contact (smooth curve) and typical mechanical contact (irregular curves).

point of the amount of inductive energy which is available to be dissipated into the arcing contact circuit, with attendant surges and contact erosion.

1.2 *Objectives*

This paper aims to present these relationships in general form, with enough experimental data to verify the analysis. Some specific fields of relay and circuit design where immediate applications are expected, and which were an incentive for this study, will now be summarized.

(i) The general definition of the "ideal" contact surges. It is found that all variations are definable in terms of two dimensionless ratios: $\beta = CR^2/\mathcal{P}N^2$, the "load design factor," and G_2/G_1 or the ratio of secondary to primary coil constants (summarized in Table I and further described below). The surge equations can then be used to predict such variations as peak voltage, amplitude and frequency of oscillations, rise time, or degree of damping. The analysis also shows that the response is oscillatory between two particular values of β, with overdamped behavior above or below these values.

(ii) An understanding of how the coil's stored inductive energy is released. Relationships are found which determine that part consumed in internal and external dissipative losses, and that part which goes into capacitive energy storage from which it may be discharged into erosion-producing arcs.

(iii) A fuller understanding of that portion of the coil's stored inductive energy that can be released during the transient period, the major features of which depend on (a) the incremental permeance of the static demagnetization curve at the releasing point, and (b) the energy replenishment from the battery during each arc breakdown interval. This is especially important in the study of contact erosion.

(iv) An explanation of some hitherto "anomalous" results. Among these are: (a) A quantitative picture of releasable coil energy as influenced by "stop-pin" height; it is shown here to be related directly to the degree of coil saturation, in accord with experience, rather than to the total stored energy as had previously been suggested. (b) A quantitative picture of the oscillations which occur with "copper-sleeve" relays. This is found to be related to that portion of the main winding which is uncoupled to the secondary.

TABLE I—CIRCUIT CONSTANTS

V_o = Battery voltage.
V_c = Instantaneous voltage across contacts.
I_o = Steady state current = V_o/R_w.
i_1, i_2 = Instantaneous current in primary or secondary circuits respectively.
q_1 = Instantaneous charge on capacitor.
N_1, N_2 = Turns in primary, or secondary, respectively.
R_w, R_2 = Resistance of primary, or secondary, winding respectively.
R_n = Primary circuit resistance external to coil (i.e., resistance of RC network).
R_1 = Total resistance of primary circuit = $R_w + R_n$.
G_1, G_2 = Coil constant for primary or secondary circuit
= $\dfrac{N_1^2}{R_1} \dfrac{N_2^2}{R_2}$ respectively (mho).
G_e = Eddy current constant of core (for which $N_2 = 1$).
[Note that $\dfrac{1}{G_1} = \dfrac{R_w + R_n}{N_1^2} = \dfrac{1}{G_w} + \dfrac{1}{G_n}$.]
L_1, L_2 = Incremental inductance of primary or secondary $N_1^2\mathcal{P}$, $N_2^2\mathcal{P}$ respectively.
$\mathcal{P}$ = Incremental permeance of coil magnetic circuit at specified magnetization (i.e., corresponding to operated ampere-turns).
C = Capacitance across load coil.
Φ = Magnetic flux.

	General Case	Case for $R_n = 0$	Case for $G_2 = 0$	Case for $G_2 = 0$ and $R_n = 0$
R' = Effective Resistance	$R_1 + \dfrac{G_2\mathcal{P}}{C}$ or $R_1(1 + \dfrac{G_2/G_1}{\beta_1})$	$R_w + \dfrac{G_2\mathcal{P}}{C}$ or $R_w(1 + \dfrac{G_2/G_w}{\beta_w})$	R_1	R_w
L' = Effective Inductance	$L_1(1 + G_2/G_1)$	$L_1(1 + G_2/G_w)$	L_1	L_1
β = Load Design Factor	$\beta_1 = \dfrac{CR_1^2}{\mathcal{P}N_1^2}$	$\beta_w = \dfrac{CR_w^2}{\mathcal{P}N_1^2}$	β_1	β_w

(v) The ability to make design estimates for a number of applications. Examples are: (a) Number and frequency of breakdowns in a "B" type transient, and the energy available for causing erosion. (b) Peak value of the final surge, following a "B" type transient as for the tail of the irregular curve in Fig. 1. This is needed in verifying whether wiring insulation will be damaged when coils with large numbers of turns are disconnected. (c) Choice of proper test values for use in the production testing of relay coils to determine whether their internal insulation

breakdown strength is satisfactory. (For this test, which has been in use on an empirical basis for many years, the energized coil circuit is interrupted by an "ideal" vacuum tube "switch"; if the coil's self-induced voltage causes an internal breakdown, the coil is rejected as an incipient service failure because of faulty insulation or lead configuration.) (d) The ability to reinterpret inconclusive data from past contact tests, or to better define tests made years ago so that their applicability to today's designs in today's circuits may be better understood.

(vi) Assessment of the mutual impact of contact erosion and relay miniaturization. For example, a smaller relay coil usually means less energy for the contact to control and therefore a smaller contact volume for a given contact life. A smaller contact volume means less wear allowance in the relay's armature motion, and hence a lower mechanical work requirement, with a correspondingly smaller relay magnet. Thus a knowledge of the interaction between the relay's inductive energy and the resulting contact wear can be an important guide to design for minimal relay sizes for a switching system where all the relays are of the same basic structure (i.e., the contacts of one relay control the winding of another).

The paper is divided into three major sections: Analysis, Experiment, and Discussion. The circuit is first analyzed in general terms, giving results which for some cases are considered too complex for further treatment in this study. Substitutions are then made which considerably simplify the equations and lead to detailed answers for the important practical case of the unprotected relay coil. The major experimental results and discussion relate to this case.

II. ANALYSIS

In this section, we shall (i) develop the circuit equations and apply them to the consideration of special situations such as (ii) critical damping, (iii) peak voltage, and (iv) energy relationships.

2.1 Development of the Circuit Equations

This section defines a circuit model, presents the loop equations, and gives the resulting solution for current in the main circuit. This value of current as a function of time is then used to derive the related values of charge, contact voltage, and rate of change of voltage.

2.1.1 *Choice of Circuit Model*

A simple relay winding shunted by an *RC* network, being connected or disconnected from a battery by means of an ideal contact, was chosen for the study. As only the surge on disconnection is studied, the influence of wiring can be included in the capacitive term, and so the results are generally applicable whether connections between contact and relay are very short, as on a printed wiring board, or quite long, as through a considerable loop of switchboard cabling. Reflections and surge impedance of the wiring are important in considering the individual showering arcs, as has been done for example in recent work of G. W. Mills[10] and J. R. Pharney;[11] but these features are outside the scope of the present study.

After some initial experiments, it was found that an adequate representation of an actual relay control circuit required the recognition of: (*i*) the distributed capacitance of the coil; (*ii*) a coupled secondary winding to represent core losses, copper sleeves, etc.; (*iii*) an effective lumped inductance representing the region of the demagnetization curve that is active during the initial surge; and (*iv*) (under certain conditions) a portion of the main winding which is not coupled with the core or secondary winding. The resulting study circuit is seen in Fig. 2a. For example, (*i*) it was found that distributed capacitance of typical relay coils is in the vicinity of 100–200 pF, which is too large
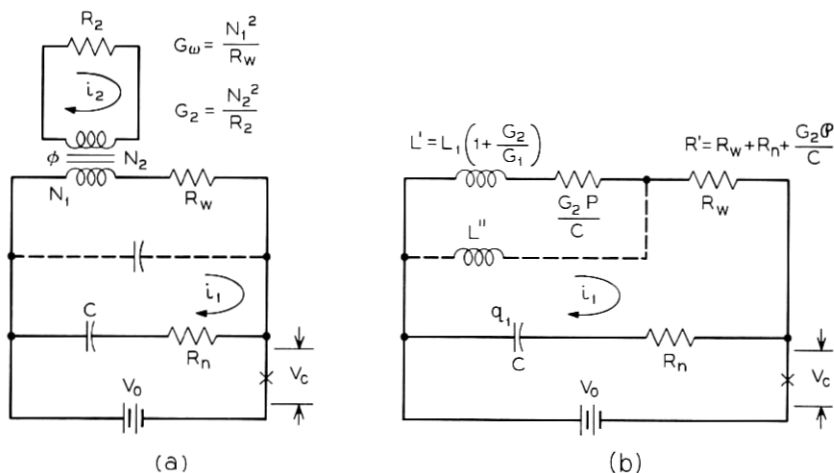

Fig. 2—Circuits for fully representing a relay as a contact load. (a) Circuit chosen for analysis. (b) Transformed circuit.

to ignore. Likewise, (ii) it was found that the discharges of typical relay structures can be so fast that the core losses (i.e., dissipation in an effective secondary winding) must be recognized. The additional influence of that portion of the coil winding which is not coupled to the "secondary" plays a significant role only when dealing with coils having a secondary consisting of a copper sleeve or short-circuited turns; it will be examined as a special case of the above circuit in Section 2.2. Following this general solution, the simpler cases are readily found as special cases; e.g., setting the protection network resistance $R_n = 0$ gives the case of an ordinary relay coil with distributed or direct shunt capacitance, setting the eddy current coil constant $G_2 = 0$ gives the case of an air core coil, or setting $C = \infty$ represents a pure resistive shunt.

The first objective is therefore to evaluate the current, charge, and contact voltage in the primary circuit for the period immediately after interrupting the circuit shown in Fig. 2a. The following considerations will be used in the initial analysis:

(i) The contact is "ideal," i.e., no gaseous or metal vapor breakdowns occur. This is in fact closely simulated by a mercury contact, and even more completely by certain vacuum tubes and transistors.

(ii) Perfect coupling is assumed between primary and secondary.

(iii) The initial conditions (just prior to $t = 0$) are that the steady current is $I_o = (V_o/R_w)$,* and the capacitor is charged to the value $-V_o$.

(iv) The flux Φ which is linked to both primary and secondary windings is proportional to the algebraic sum of the instantaneous ampere turns of primary and secondary, in accordance with the usual magnetic circuit concepts.

(v) The inductance of the load can be represented by a lumped value which effectively simulates the flux-current relation in the coil's working region. Use of a lumped-constant term simplifies the circuit equations, which otherwise become very difficult to solve in simple forms. The meaning of a lumped-constant inductance is better understood with the help of Fig. 3, which shows the static flux-ampere turn characteristic of a typical relay magnet for operating and releasing cycles. For the present case, the releasing cycle, or demagnetization curve, applies. The instantaneous inductance is the slope of
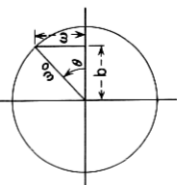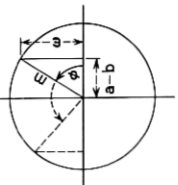
---

* For definitions of terms, see Tables I, II, and III.

TABLE II—CONSTANTS APPEARING IN EQUATIONS

CONST.	GENERAL EXPRESSION	VALUE WHEN $R_n = 0$	VALUE WHEN $G_2 = 0$	VALUE WHEN $\begin{cases}R_n=0\\G_2=0\end{cases}$
$K =$	$\dfrac{1+G_2/G_w}{1+G_2/G_1}$	$=1$	$=1$	$=1$
$a =$	$\dfrac{R_w}{L_1(1+G_2/G_w)} = \dfrac{R_w}{KL'}$	$=\dfrac{R_w}{L_1(1+G_2/G_w)} = \dfrac{R_w}{L'}$	$=\dfrac{R_w}{L_1} = \dfrac{R_w}{N_1^2\vartheta} = \dfrac{1}{G_w\vartheta}$	$=\dfrac{R_w}{L_1} = \dfrac{R_w}{N_1^2\vartheta} = \dfrac{1}{G_w\vartheta} = 2b$
$b =$	$\dfrac{R_1'}{2L'} = \dfrac{R_1 + \frac{G_2\vartheta}{C}}{2L_1(1+G_2/G_1)} = \dfrac{1+\frac{G_2/G_1}{\beta_1}}{2G_1\vartheta(1+G_2/G_1)}$	$\dfrac{R_w + \frac{G_2\vartheta}{C}}{2L_1(1+G_2/G_w)} = \dfrac{1+\frac{G_2/G_w}{\beta_w}}{2G_w\vartheta(1+G_2/G_w)}$	$\dfrac{R_1}{2L'} = \dfrac{R_1}{2N_1^2\vartheta} = \dfrac{1}{2G_1\vartheta}$	$\dfrac{R_w}{2L_1} = \dfrac{R_w}{2N_1^2\vartheta} = \dfrac{1}{2G_w\vartheta}$
$(a-b) =$	$\dfrac{1}{2L'}\left[R_w - \dfrac{G_2\vartheta}{C} - R_n\dfrac{1-G_2/G_w}{1+G_2/G_w}\right]$ $= \dfrac{\frac{R_w}{R_1} - \frac{G_2/G_1}{\beta_1} - \frac{R_n(1-G_2/G_w)}{R_1(1+G_2/G_w)}}{2G_1\vartheta(1+G_2/G_1)}$	$\dfrac{1}{2L'}\left[R_w - \dfrac{G_2\vartheta}{C}\right]$ $= \dfrac{1-\frac{G_2/G_w}{\beta_w}}{2G_w\vartheta(1+G_2/G_w)}$	$\dfrac{R_w - R_n}{2L_1}$ $\dfrac{R_w - R_n}{2N_1^2\vartheta}$	$\dfrac{R_w}{2L_1} = b$
$\omega_0 =$	$\dfrac{1}{\sqrt{L'C}} = G_1\vartheta\sqrt{\beta_1(1+G_2/G_1)}$	$\dfrac{1}{\sqrt{L'C}} = G_w\vartheta\sqrt{\beta_w(1+G_2/G_w)}$	$\dfrac{1}{\sqrt{L'C}} = \dfrac{1}{N_1\sqrt{\vartheta C}}$	$\dfrac{1}{\sqrt{L_1C}} = \dfrac{1}{N_1\sqrt{\vartheta C}}$
$\omega =$	$\sqrt{\omega_0^2-b^2} =$ $\dfrac{\sqrt{4L'^2C-C^2\left(R_1+\frac{G_2\vartheta}{G}\right)^2}}{2L'C} = \dfrac{\sqrt{\frac{4}{\beta_1}-\left(1-\frac{G_2/G_1}{\beta_1}\right)^2}}{2G_1\vartheta(1+G_2/G_1)}$ $= \dfrac{\sqrt{4N_1^2\vartheta C\left(1+\frac{G_2}{2G_1}\right)-C^2R_1^2-G_2^2\vartheta^2}}{2L'C}$	$\dfrac{1}{\sqrt{L'C}} = G_w\vartheta\sqrt{\beta_w(1+G_2/G_w)}$ $\dfrac{\sqrt{4L'^2C-C^2\left(R_w+\frac{G_2\vartheta}{C}\right)^2}}{2L'C} = \dfrac{\sqrt{\frac{4}{\beta_w}-\left(1-\frac{G_2/G_w}{\beta_w}\right)^2}}{2G_w\vartheta(1+G_2/G_w)}$ $= \dfrac{\sqrt{4N_1^2\vartheta C\left(1+\frac{G_2}{2G_w}\right)-C^2R_w^2-G_2^2\vartheta^2}}{2L'C}$	$\dfrac{1}{\sqrt{L'C}} = \dfrac{1}{N_1\sqrt{\vartheta C}}$ $\dfrac{\sqrt{4L_1^2C-C^2R_1^2}}{2L_1C} = \dfrac{\sqrt{\frac{4}{\beta_1}-1}}{2G_1\vartheta}$ $\dfrac{\sqrt{4N_1^2\vartheta C-C^2R_1^2}}{2L_1C}$	$\dfrac{1}{\sqrt{L_1C}} = \dfrac{1}{N_1\sqrt{\vartheta C}}$ $\dfrac{\sqrt{4L_1^2C-C^2R_w^2}}{2L_1C} = \dfrac{\sqrt{\frac{4}{\beta_w}-1}}{2G_w\vartheta}$ $\dfrac{\sqrt{4N_1^2\vartheta C-C^2R_w^2}}{2L_1C}$
$m =$	$\dfrac{\omega_0}{1+G_2/G_w}\sqrt{1+G_2/G_w - \dfrac{CR_n}{G_w\vartheta}}$	$\dfrac{\omega_0}{\sqrt{1+G_2/G_w}}$	$\omega_0\sqrt{1-\dfrac{CR_n}{G_w\vartheta}}$	$=\omega_0$

TABLE III—EXPRESSIONS INVOLVING PHASE ANGLE

VARIABLE	GENERAL EXPRESSION	VALUE WHEN $R_n = 0$	VALUE WHEN $G_2 = 0$	VALUE WHEN $\begin{cases} R_n = 0 \\ G_2 = 0 \end{cases}$	VALUES OF θ & ϕ
$\sin\theta =$	$\dfrac{\omega}{\omega_0} = \sqrt{1 - \dfrac{b^2}{\omega_0^2}} = \sqrt{\dfrac{\dfrac{4}{\beta_1} - \left(1 - \dfrac{G_2/G_1}{\beta_1}\right)^2}{4(1+G_2/G_1)}}$	$\sqrt{\dfrac{\dfrac{4}{\beta_W} - \left(1 - \dfrac{G_2/G_W}{\beta_W}\right)^2}{4(1+G_2/G_W)}}$	$=\sqrt{1 - \dfrac{\beta_1}{4}}$	$=\sqrt{1 - \dfrac{\beta_W}{4}}$	
$\cos\theta =$	$\dfrac{b}{\omega_0} = \dfrac{CR_1 + G_2\mathscr{P}}{2\sqrt{CN_1{}^2\mathscr{P}\,(1+G_2/G_1)}} = \dfrac{\sqrt{\dfrac{G_2/G_1}{\beta_1}}\left(1 + \dfrac{G_2/G_1}{\beta_1}\right)}{2\sqrt{1+G_2/G_1}}$	$=\dfrac{CR_W + G_2\mathscr{P}}{2\sqrt{CN_1{}^2\mathscr{P}\,(1+G_2/G_W)}} = \dfrac{\sqrt{\dfrac{G_2/G_W}{\beta_W}}\left(1+\dfrac{G_2/G_W}{\beta_W}\right)}{2\sqrt{1+G_2/G_W}}$	$=\dfrac{\sqrt{\beta_1}}{2} = \dfrac{1}{2}\dfrac{R_1}{N_1}\sqrt{\dfrac{C}{\mathscr{P}}}$	$=\dfrac{\sqrt{\beta_W}}{2} = \dfrac{1}{2}\dfrac{R_W}{N_1}\sqrt{\dfrac{C}{\mathscr{P}}}$	
$\tan\theta =$	$\dfrac{\omega}{b} = \sqrt{\dfrac{\dfrac{4}{\beta_1} - \left(1 - \dfrac{G_2/G_1}{\beta_1}\right)^2}{1 + \dfrac{G_2/G_1}{\beta_1}}} = \sqrt{\dfrac{\dfrac{4}{\beta_W} - \left(1 - \dfrac{G_2/G_W}{\beta_W}\right)^2}{1 + \dfrac{G_2/G_W}{\beta_W}}}$		$=\sqrt{\dfrac{4 - \beta_1}{\beta_1}}$	$=\sqrt{\dfrac{4 - \beta_W}{\beta_W}}$	
$\sin\phi =$	$\dfrac{\omega}{m} = \dfrac{1 + G_2/G_W - \dfrac{CR_n}{G_W\mathscr{P}}}{\sqrt{1 + G_2/G_W - \dfrac{CR_n}{G_W\mathscr{P}}}} \sin\theta$	$=\sqrt{1 + G_2/G_W}\;\sin\theta$	$=\dfrac{\sin\theta}{\sqrt{1 - \dfrac{CR_n}{G_W\mathscr{P}}}}$	$=\sin\theta$	
$\cos\phi =$	$\dfrac{a-b}{m} = \dfrac{2\sqrt{\beta_1(1+G_2/G_W)}\left[\dfrac{R_W}{R_1} - \dfrac{G_2/G_1}{\beta_1} - \dfrac{R_n(1-G_2/G_W)}{R_1(1+G_2/G_W)}\right]}{\sqrt{1+G_2/G_W - \dfrac{CR_n}{G_W\mathscr{P}}}\left(1 + \dfrac{G_2/G_1}{\beta_1}\right)}$ = $\dfrac{\left[\dfrac{R_W}{R_1} - \dfrac{G_2/G_1}{\beta_1} - \dfrac{R_n(1-G_2/G_W)}{R_1(1+G_2/G_W)}\right]}{\sqrt{1 + G_2/G_W - \dfrac{CR_n}{G_W\mathscr{P}}}\left(1 + \dfrac{G_2/G_1}{\beta_1}\right)}\cos\theta$	$\dfrac{\left(1 - \dfrac{G_2/G_W}{\beta_W}\right)}{1 + \dfrac{G_2/G_W}{\beta_W}}\sqrt{1 + \dfrac{G_2}{G_W}}\cos\theta$	$\dfrac{R_W - R_n}{R_1}\sqrt{1 - \dfrac{CR_n}{G_W\mathscr{P}}}\cos\theta$	$=\cos\theta$	
$\tan\phi =$	$\dfrac{\omega}{a-b} = \dfrac{\left[\dfrac{R_W}{R_1} - \dfrac{G_2/G_1}{\beta_1} - \dfrac{R_n(1-G_2/G_W)}{R_1(1+G_2/G_W)}\right]}{\left[\dfrac{R_W}{R_1} - \dfrac{G_2/G_1}{\beta_1} - \dfrac{R_n(1-G_2/G_W)}{R_1(1+G_2/G_W)}\right]}$ = $\dfrac{\sqrt{\dfrac{4}{\beta_1} - \left(1 - \dfrac{G_2/G_1}{\beta_1}\right)^2}}{\dfrac{R_W}{R_1} - \dfrac{G_2/G_1}{\beta_1} - \dfrac{R_n(1-G_2/G_W)}{R_1(1+G_2/G_W)}}$	$\dfrac{\left(1 + \dfrac{G_2/G_W}{\beta_W}\right)}{\left(1 - \dfrac{G_2/G_W}{\beta_W}\right)}\tan\theta$	$\dfrac{R_1}{R_W - R_n}\tan\theta$	$=\tan\theta$	

NOTE:
VALUES IN THIS TABLE ARE FOR $\omega_0{}^2 > b^2$; WHEN $b^2 > \omega_0{}^2$, SUBSTITUTE $\sinh$, $\cosh$, $\tanh$ FOR $\sin$, $\cos$, TAN RESPECTIVELY. WHEN $\omega_0 = b$, SEE TABLE XI.
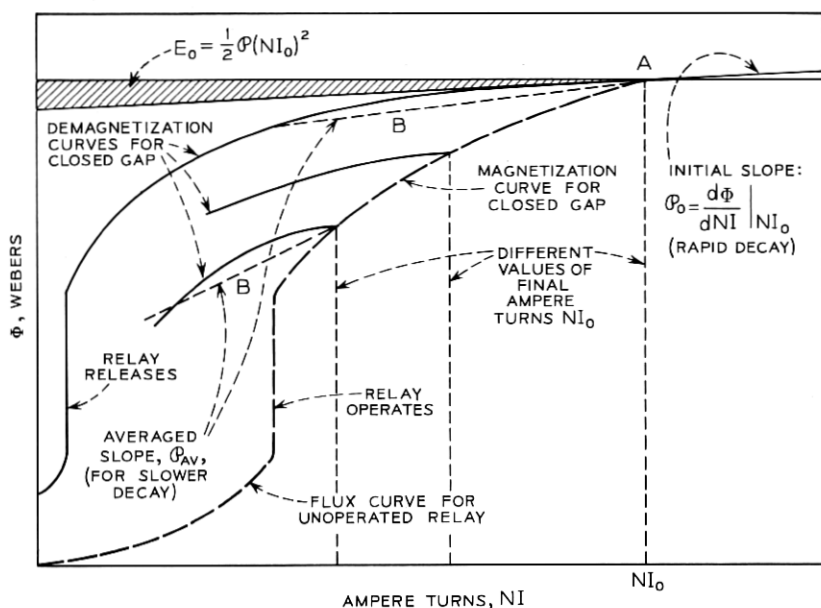
WHEN $a \geqq b$, $0 < \phi \leqq \dfrac{\pi}{2}$; WHEN $b > a$, $\dfrac{\pi}{2} < \phi \leqq \pi$

Fig. 3—Representation of inductance, $L = \mathcal{P}N^2$, when contact opens a relay coil circuit.

this demagnetization curve in the applicable working range, and may be expressed as

$$L = \mathcal{P}N^2$$

where $\mathcal{P} = (d\Phi/dNI) \mid_{NI_o}$, N = number of turns in the coil, and NI_o = ampere turns at the operated point (i.e., starting point of the demagnetization curve on disconnection). $\mathcal{P}$ is the differential permeance, or slope of the demagnetization curve, over the region where flux is changing during the surge. In the case of very fast surges, the flux is substantially unchanged during the surge, and the value of $\mathcal{P}$ at NI_o applies, as shown at A in Fig. 3. For slower surges, a larger value of $\mathcal{P}$ representing an average slope over the working range, as indicated by the dotted lines B in the figure, is presumed to apply. Values of $\mathcal{P}$ are further discussed in Section 3.1.2.

The analysis has been developed around this general circuit. The resulting general solution, which involves an appreciable number of variables, is relatively complex and its detailed examination is reserved for later computer-assisted studies. For the present study, special

attention is aimed only at the simpler but important practical case of the ordinary unprotected relay, which involves only a simple capacitive shunt, a term which is always needed if only to cover the inevitable distributed capacitance of the coil itself. In addition, the manner in which the general expressions reduce to simpler forms, by neglecting appropriate terms, will be noted; conformity to previously known solutions for the conventional L, R, C circuit affords at least partial confirmation of the general analysis. The special cases chosen for detailed consideration are:

$R_n = 0$, G_2 finite (relay coil with capacitive shunt),

R_n finite, $G_2 = 0$ (air core coil with RC shunt), and

$R_n = 0$, $G_2 = 0$ (air core coil with capacitive shunt).

The appropriate expressions for each of these cases are tabulated in the accompanying tables.

The symbols applicable to this model circuit are summarized in Table I. The notation using terms $G = N^2/R$ for coil constant, and expressing inductance in terms of turns and permeance $\mathcal{P}$ $(L = \mathcal{P}N^2)$, has been used because of its convenience and common use in relay design. The resulting equations are also considerably simplified by their use.

2.1.2 Equations for Current in Primary

The equations for the model circuit, Fig. 2a, are derived in Appendix A. The procedure was to sum the voltages around primary and secondary circuits, respectively, using the flux common to both windings to determine the inductive terms, $N_1(d\Phi/dt)$ and $N_2(d\Phi/dt)$. LaPlace Transform techniques were used to represent the initial conditions and obtain the solution for current i_1 in the primary circuit. The three possible solutions, oscillatory, critically damped, or overdamped [i.e., ω_o^2 greater than, equal to, or less than b^2] are:

Case I:
Oscillatory
$$i_1 = \frac{Ki_o e^{-bt} \sin(\omega t + \varphi)}{\sin \varphi} \qquad (\omega_o^2 < b^2)$$

Case II:
Critically
Damped
$$i_1 = Ki_o e^{-bt}[1 + (a - b)t] \qquad (\omega_o^2 = b^2) \qquad (1)$$

Case III:
Overdamped
$$i_1 = \frac{Ki_o e^{-bt} \sinh(\omega t + \varphi)}{\sinh \varphi} \qquad (\omega_o^2 > b^2).$$

The values of the constants, of the phase angles, and of related terms, are summarized in Tables II and III respectively. The circuit equations

also showed that the transformed circuit of Fig. 2b could be used to represent all the variations in the primary circuit, where the primed values of L and R represent the effective values of primary circuit inductance and resistance respectively. This simplification results from the term $G_2 \mathcal{P}/C$, which is found to represent the dissipative losses due to the secondary. (The term L'' will be discussed in Section 2.2.2.)

2.1.3 *Equations for Charge, Current, and Contact Voltage*

The expression for current, equation (1), may be used to derive equations for charge and contact voltage as a function of time. The charge q_1 is given by

$$q_1 = \int i_1 \, dt \tag{2}$$

and contact voltage by

$$V_c = V_o + \frac{q_1}{C} + i_1 R_n \ . \tag{3}$$

The resulting general expressions for all these variables are summarized in Table IV for the cases: oscillatory, critically damped, and over-damped. Equations are also given for two important special cases: $R_n = 0$, and both R_n and $G_2 = 0$ (i.e., capacitive shunt only, or air core coil, respectively.) Of course, other special cases can be derived by making appropriate substitutions into the general equations. Table V similarly summarizes these results for the instant of contact opening, i.e., for conditions at $t = 0$. It is found that, at $t = 0$, Cases I, II, or III all give equal values for each variable, as one would expect.

The equations in Table IV express the variations in charge, current, and contact voltage as a function of time. Of these, it is often of greatest interest to consider the contact voltage; a normalized version is plotted in Fig. 8 based on the discussion of peak voltages in Section 2.3.

2.2 *Discussion of Conditions at Critical Damping*

The boundary condition for critical damping, now to be considered, helps to explain the way in which the various kinds of surges are influenced by the circuit parameters. Comparison of experimentally observed conditions at the critical damping point with this analysis also provides confirmation for much of the analysis; these measurements also provide means for determining effective values for the core loss

TABLE IV—BASIC CIRCUIT EQUATIONS

VARIABLE		COLUMN 1 GENERAL CASE	COLUMN 2 WHEN $R_n = 0$	COLUMN 3 WHEN $\begin{cases} R_n = 0 \\ G_2 = 0 \end{cases}$	
CASE I					**CASE I**
(a)	$q_1 =$	$-\dfrac{KI_0 e^{-bt}}{\omega_0 \sin\phi} \sin(\omega t + \phi + \theta)$	$= -\dfrac{CV_0 \beta_w^{-1/2} e^{-bt}}{\sin\theta} \sin(\omega t + \phi + \theta)$	$= -\dfrac{CV_0 \beta_w^{-1/2} e^{-bt}}{\sin\theta} \sin(\omega t + 2\theta)$	q_1
(b)	$i_1 =$	$\dfrac{KI_0 e^{-bt}}{\sin\phi} \sin(\omega t + \phi)$	$= \dfrac{I_0 e^{-bt}}{\sin\theta} \sin(\omega t + \phi)$	$= \dfrac{I_0 e^{-bt}}{\sin\theta} \sin(\omega t + \theta)$	i_1
(c)	$V_c - V_0 =$	$\dfrac{KI_0 e^{-bt}}{\sin\phi}\left[R_n \sin(\omega t + \phi) - \dfrac{1}{\omega_0 C} \sin(\omega t + \phi + \theta)\right]$	$= -\dfrac{V_0 \beta_w^{-1/2} e^{-bt}}{\sin\theta} \sin(\omega t + \phi + \theta)$	$= -\dfrac{V_0 \beta_w^{-1/2} e^{-bt}}{\sin\theta} \sin(\omega t + 2\theta)$	$V_c - V_0$
(d)	$\dot{V}_c =$	$\dfrac{KI_0 e^{-bt}}{\sin\phi}\left[\dfrac{1}{C}\sin(\omega t + \phi) - \omega_0 R_n \sin(\omega t + \phi - \theta)\right]$	$= \dfrac{I_0 e^{-bt}}{C \sin\phi}\sin(\omega t + \phi)$	$= \dfrac{I_0 e^{-bt}}{C \sin\phi}\sin(\omega t + \theta)$	$\dot{V}_c$
CASE II					**CASE II**
(a)	$q_1 =$	$-CV_0 e^{-bt}\left[1 + \dfrac{b(a-b)}{a}t\right]$	$= -CV_0 e^{-bt}\left[1 + \dfrac{b(a-b)}{a}t\right]$	$= -CV_0 e^{-bt}\left(1 + \dfrac{bt}{2}\right)$	q_1
(b)	$i_1 =$	$KI_0 e^{-bt}\left[1 + (a-b)t\right]$	$= I_0 e^{-bt}\left[1 + (a-b)t\right]$	$= I_0 e^{-bt}(1 + bt)$	i_1
(c)	$V_c - V_0 =$	$-V_0 e^{-bt}\left[1 - \dfrac{KR_n}{R_w} + (a-b)\left(\dfrac{b}{a} - \dfrac{KR_n}{R_w}\right)t\right]$	$= -V_0 e^{-bt}\left[1 + \dfrac{b(a-b)}{a}t\right]$	$= -V_0 e^{-bt}\left(1 + \dfrac{bt}{2}\right)$	$V_c - V_0$
(d)	$\dot{V}_c =$	$\dfrac{KI_0 e^{-bt}}{C}\left[1 - CR_n(2b-a) + (a-b)(1-bCR_n)t\right]$	$= \dfrac{I_0}{C}e^{-bt}\left[1 + (a-b)t\right]$	$= \dfrac{I_0}{C}e^{-bt}(1 + bt)$	$\dot{V}_c$
CASE III					**CASE III**
(a)	$q_1 =$	$-\dfrac{KI_0 e^{-bt}}{\omega_0 \sinh\phi}\sinh(\omega t + \phi + \theta)$	$= -\dfrac{CV_0 \beta_w^{-1/2} e^{-bt}}{\sinh\theta}\sinh(\omega t + \phi + \theta)$	$= -\dfrac{CV_0 e^{-bt}}{\sinh\theta}\sinh(\omega t + 2\theta)$	q_1
(b)	$i_1 =$	$\dfrac{KI_0 e^{-bt}}{\sinh\phi}\sinh(\omega t + \phi)$	$= \dfrac{I_0 e^{-bt}}{\sinh\theta}\sinh(\omega t + \phi)$	$= \dfrac{I_0 e^{-bt}}{\sinh\theta}\sinh(\omega t + \theta)$	i_1
(c)	$V_c - V_0 =$	$\dfrac{KI_0 e^{-bt}}{\sinh\phi}\left[R_n \sinh(\omega t + \phi) - \dfrac{1}{\omega_0 C}\sinh(\omega t + \phi + \theta)\right]$	$= -\dfrac{V_0 \beta_w^{-1/2} e^{-bt}}{\sinh\theta}\sinh(\omega t + \phi + \theta)$	$= -\dfrac{V_0 e^{-bt}}{\sinh\theta}\sinh(\omega t + 2\theta)$	$V_c - V_0$
(d)	$\dot{V}_c =$	$\dfrac{KI_0 e^{-bt}}{\sinh\phi}\left[\dfrac{1}{C}\sinh(\omega t + \phi) - \omega_0 R_n \sinh(\omega t + \phi - \theta)\right]$	$= \dfrac{I_0 e^{-bt}}{C \sinh\phi}\sinh(\omega t + \phi)$	$= \dfrac{I_0 e^{-bt}}{C \sinh\phi}\sinh(\omega t + \theta)$	$\dot{V}_c$

TABLE V—BASIC CIRCUIT EQUATIONS WHEN $t = 0^+$

Variable	General Case	Case when $R_n = 0$
(a) $q_1 =$	$-CV_o$	$= -CV_o$
(b) $i_1 =$	KI_o	$= I_o$
(c) $V_c =$	KI_oR_n	$= 0$
(d) $\dot{V}_c =$	$\dfrac{K^2I_o}{C}\left[1 - \dfrac{CR_n^2}{L_1(1 + G_2/G_w)_2}\right]$	$= \dfrac{I_o}{C}$

term, G_2, and the effective permeance, $\mathcal{P}$, of the core, as will be seen in Section 3.2.

2.2.1 General Expressions

The critically damped condition is $\omega_0^2 = b^2$, or alternatively:

$$\frac{CR'^2}{4L'} = 1. \tag{4}$$

Substituting values for R' and L' from Table I,

$$C\left(\frac{G_2\mathcal{P}}{C} + R_1\right)^2 = 4N_1^2\mathcal{P}(1 + G_2/G_1).$$

This expression is simplified by making the substitution

$$\beta_1 = \frac{CR_1^2}{\mathcal{P}N_1^2},$$

yielding a quadratic equation which can be expressed in terms of only two variables, β_1 and G_2/G_1. The solution is given by either of the two equivalent expressions, equations (5a) and (5b), of which the former is usually more convenient:

$$G_2/G_1 = \beta_1^{\frac{1}{2}}(\beta_1^{\frac{1}{2}} \pm 2) \tag{5a}$$

or

$$\beta_1 = 2\left[1 + \frac{G_2}{2G_1} \pm \left(1 + \frac{G_2}{G_1}\right)^{\frac{1}{2}}\right]. \tag{5b}$$

These equations have two solutions, which depend on whether $G_2/G_1 > \beta_1$, or $G_2/G_1 < \beta_1$. The two solutions are plotted in Fig. 4, for the range of these values likely to be encountered in relay switching

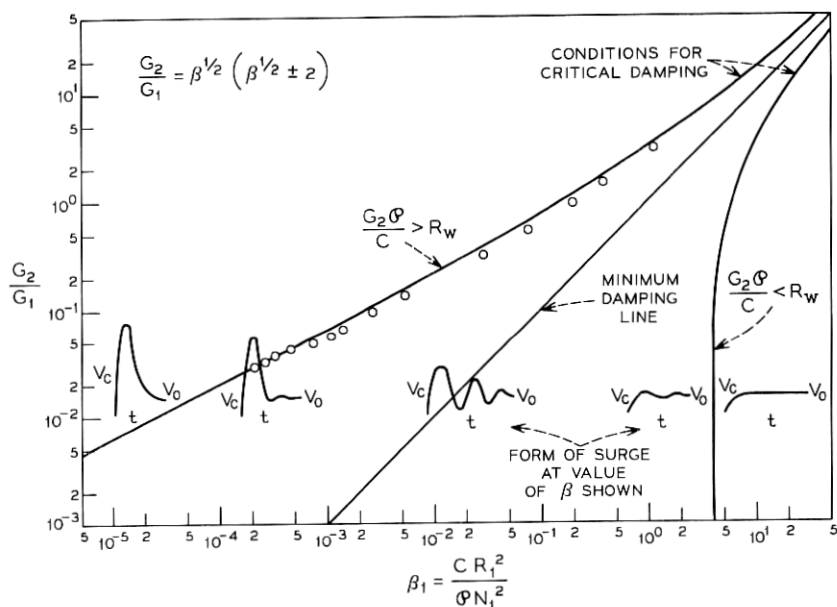Fig. 4—Conditions for critical damping—G_2/G_1 vs β.*

practice. Thus, the boundary between oscillatory and overdamped conditions is determined by either of two circumstances:

(i) Losses in *secondary* circuit are dominant [use + sign in equation (5a) or − sign in equation (5b)], for which

$$\frac{G_2}{G_1} > \beta_1 , \quad \text{or} \quad \frac{G_2 \mathcal{P}}{C} > R_1 .$$

Here,

$$\frac{G_2}{G_1} = \beta_1^{\frac{1}{2}}(\beta_1^{\frac{1}{2}} + 2) \tag{6a}$$

or

$$\beta_1 = 2\left[\left(1 + \frac{G_2}{2G_1}\right) - \left(1 + \frac{G_2}{G_1}\right)^{\frac{1}{2}}\right] \tag{6b}$$

and there are positive values of G_2/G_1 for all positive values of β_1 .

---

* The subscripts "1" or "w", applied to G and β in various figures, are used to call attention to the applicability of the information; e.g., β_1 indicates that the general analysis (including RC network) applies; β_w indicates the analysis specifically applied to the unprotected case, where $R_n = 0$.

(*ii*) Losses in *primary* circuit are dominant [use $-$ sign in equation (5a) or $+$ sign in equation (5b)], for which

$$\frac{G_2}{G_1} < \beta_1 , \quad \text{or} \quad R_1 > \frac{G_2 \mathcal{P}}{C}.$$

Here,

$$\frac{G_2}{G_1} = \beta_1^{\frac{1}{2}}(\beta_1^{\frac{1}{2}} - 2) \tag{7a}$$

or

$$\beta_1 = \left[1 + \frac{G_2}{2G_1} + \left(1 + \frac{G_2}{G_1}\right)^{\frac{1}{2}}\right] \tag{7b}$$

and meaningful (i.e., positive) values of G_2/G_1 only exist when $\beta_1 > 4$.

Note that, when $G_2 = 0$, i.e., there are no eddy current losses, then from equation (5b),

$$\beta_1 = 4$$

as is well known for the conventional L, R, C circuit.

The condition

$$\frac{G_2}{G_1} = \beta_1 \left(\text{or} \quad \frac{G_2 \mathcal{P}}{C} = R_1\right)$$

is seen to be incompatible with critical damping. It is indicated by the 45-degree line in Fig. 4 which in fact corresponds to the point of minimum damping. The character of the contact voltage surges in the various regions is sketched on the figure, summarized as follows. For a given value of G_2/G_1, the response will be oscillatory for values of β_1 lying between the two curves, with minimum damping when $\beta_1 = G_2/G_1$. When β_1 equals or exceeds the value delineated by the right-hand curve, the response will be critically damped or overdamped with a gradual asymptotic rise to V_o. When β_1 equals or is less than the value delineated by the left-hand curve, the response will be critically damped or overdamped with a single overshoot followed by an asymptotic decay to V_o.

Since the principal variation in β_1 is usually the result of variations in C, it is also useful to replot Fig. 4 in the form G_2/G_1 vs C, for a range of values of $(N_1/R_1)^2 \mathcal{P}$. Such a family of curves is given in Fig. 5. It is sometimes helpful to analyze experimental data by plotting the points on such a graph.
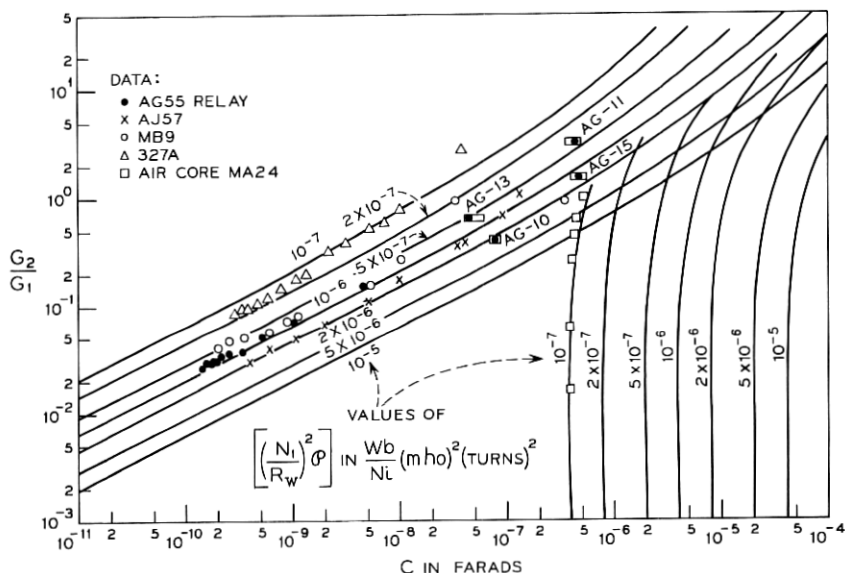
Fig. 5—Conditions for critical damping—G_2/G_1 vs C.

The data points seen in Figs. 4 and 5 will be explained in the later discussion of experimental results, Section 3.2.

The critically damped circuit equations, Case II in Table IV, may now be extended to include expressions for the two-valued equalities of equation (5), which were not previously obvious. For this purpose it is convenient to make available the related values of some of the terms appearing in these equations. In the present study we consider only the simpler cases for $R_n = 0$, or both R_n and $G_2 = 0$, which are summarized in Table VI. Using these equalities, the critically damped circuit equations of Table IV can be simplified for easier handling, as given for reference purposes in Table VII.

The predicted boundaries between overdamped and oscillatory conditions shown in Figs. 4 and 5 afford a convenient means for experimentally verifying the foregoing circuit analysis. A test relay is selected which has parallel-wound primary and secondary coils. The primary is bridged by a variable capacitor, C, while the secondary is bridged by a variable resistor, R_2'. For a chosen setting of C, the contact voltage surge V_c is observed by oscilloscope, and R_2' is varied until the surge appears to be critically damped. This process may be repeated for any desired number of settings for C, which must include corrections to include any distributed capacitance in the winding and wiring,

Constant	Core Losses Dominant i.e. $\dfrac{G_2\mathcal{P}}{C} > R_w$, or $G_2/G_w > \beta_w$ (holds for all values of $\beta_w > 0$)	Coil Losses Dominant i.e. $\dfrac{G_2\mathcal{P}}{C} < R_w$, or $G_2/G_w < \beta_w$ (holds only for values of $\beta_w \gtreqqless 4$)
$G_2/G_w =$	$\beta_w^{\frac{1}{4}}(\beta_w^{\frac{1}{4}} + 2)$	$\beta_w^{\frac{1}{4}}(\beta_w^{\frac{1}{4}} - 2)$
$1 + G_2/G_w =$	$(\beta_w^{\frac{1}{4}} + 1)^2$	$(\beta_w^{\frac{1}{4}} - 1)^2$
$\dfrac{G_2/G_w}{\beta_w} =$	$1 + 2\beta_w^{-\frac{1}{4}}$	$1 - 2\beta_w^{-\frac{1}{4}}$
$a =$	$\dfrac{1}{G_w\mathcal{P}(\beta_w^{\frac{1}{4}} + 1)^2}$	$\dfrac{1}{G_w\mathcal{P}(\beta_w^{\frac{1}{4}} - 1)^2}$
$b =$	$\dfrac{1}{G_w\mathcal{P}\beta_w^{\frac{1}{4}}(\beta_w^{\frac{1}{4}} + 1)}$	$\dfrac{1}{G_w\mathcal{P}\beta_w^{\frac{1}{4}}(\beta_w^{\frac{1}{4}} - 1)}$
$a - b =$	$-\dfrac{1}{G_w\mathcal{P}\beta_w^{\frac{1}{4}}(\beta_w^{\frac{1}{4}} + 1)^2}$	$\dfrac{1}{G_w\mathcal{P}\beta_w^{\frac{1}{4}}(\beta_w^{\frac{1}{4}} - 1)^2}$
$b/a =$	$\dfrac{\beta_w^{\frac{1}{4}} + 1}{\beta_w^{\frac{1}{4}}}$	$\dfrac{\beta_w^{\frac{1}{4}} - 1}{\beta_w^{\frac{1}{4}}}$
$\dfrac{b}{a}(a - b) =$	$-\dfrac{1}{G_w\mathcal{P}\beta_w(\beta_w^{\frac{1}{4}} + 1)}$	$\dfrac{1}{G_w\mathcal{P}\beta_w(\beta_w^{\frac{1}{4}} - 1)}$

TABLE VII—CIRCUIT EQUATIONS AT CRITICAL DAMPING (FOR THE CASE WHEN $R_n = 0$)

Variable	Core Losses Dominant i.e. $\dfrac{G_2 \mathcal{P}}{C} > R_w$, or $G_2/G_w > \beta_w$ (holds for all values of $\beta_w > 0$)	Coil Losses Dominant i.e. $\dfrac{G_2 \mathcal{P}}{C} < R_w$, or $G_2/G_w < \beta_w$ (holds only for values of $\beta_w \geqq 4$)
$q_1 =$	$-CV_o e^{-bt}\left[1 - \dfrac{t}{G_w \mathcal{P}\beta_w(\beta_w^{\frac{1}{2}} + 1)}\right]$	$-CV_o e^{-bt}\left[1 + \dfrac{t}{G_w \mathcal{P}\beta_w(\beta_w^{\frac{1}{2}} - 1)}\right]$
$i_1 =$	$I_o e^{-bt}\left[1 - \dfrac{t}{G_w \mathcal{P}\beta_w^{\frac{3}{2}}(\beta_w^{\frac{1}{2}} + 1)^2}\right]$	$I_o e^{-bt}\left[1 + \dfrac{t}{G_w \mathcal{P}\beta_w^{\frac{3}{2}}(\beta_w^{\frac{1}{2}} - 1)^2}\right]$
$V_c - V_o =$	$-V_o e^{-bt}\left[1 - \dfrac{t}{G_w \mathcal{P}\beta_w^{\frac{1}{2}}(\beta_w^{\frac{1}{2}} + 1)}\right]$	$-V_o e^{-bt}\left[1 + \dfrac{t}{G_w \mathcal{P}\beta_w^{\frac{1}{2}}(\beta_w^{\frac{1}{2}} + 1)}\right]$
$\dot{V}_c =$	$\dfrac{I_o}{C} e^{-bt}\left[1 - \dfrac{t}{G_w \mathcal{P}\beta_w^{\frac{1}{2}}(\beta_w^{\frac{1}{2}} + 1)^2}\right]$	$\dfrac{I_o}{C} e^{-bt}\left[1 + \dfrac{t}{G_w \mathcal{P}\beta_w^{\frac{1}{2}}(\beta_w^{\frac{1}{2}} - 1)^2}\right]$
where $b =$	$\dfrac{1}{G_w \mathcal{P}\beta_w^{\frac{1}{2}}(\beta_w^{\frac{1}{2}} + 1)}$	$\dfrac{1}{G_w \mathcal{P}\beta_w^{\frac{1}{2}}(\beta_w^{\frac{1}{2}} - 1)}$

as is discussed in Section 3.1. These data may then be analyzed to give estimates for G_e and $\mathcal{P}$ for the particular structure being studied; and also to compare the measured variation of G_2/G_1 vs β against the predicted values, as is discussed in Sections 3.1.3 and 3.2.

In accord with relay design practice, assume that the effective secondary coil constant, G_2, is the sum of two separate terms,

$$G_s = \frac{N_2^2}{R_2 + R_2'}$$

and G_e, representing the actual secondary winding, and the single-turn eddy current coupling term for the core, respectively. An approximate estimate of G_e may then be obtained from an examination of those data points for which G_s has quite small values. This procedure is helped by the fact that, at small values of G_2/G_1 and β, the critical damping equations (6) may be further simplified. By series expansion of equation (6b), neglecting terms of higher than second order, it reduces to

$$\beta_1 = \frac{1}{4}\left(\frac{G_2}{G_1}\right)^2 \tag{8}$$

or, from Table I,

$$G_2 = G_s + G_e = 2N_1\sqrt{C/\mathcal{P}}. \tag{9}$$

Thus, a plot of G_s vs $C^{\frac{1}{2}}$, for small values of G_2, should yield a straight line with a negative intercept equal to G_e and a slope of $2N_1\mathcal{P}^{-\frac{1}{2}}$, from which $\mathcal{P}$ may also be determined. This procedure is indicated in the experiment summarized in Table VIII, and further discussed in Section 3.1, with determination of G_e shown in Fig. 17. In this example, G_e was found to equal about 220 mho. Using this figure to obtain an approximate value for G_2, the effective value of permeance $\mathcal{P}$ (at least for small values of G_2) may then be determined using equation (9), as is also shown in Fig. 17.

2.2.2 Peak Voltages and Oscillations due to Imperfect Coupling Between Primary and Secondary

The foregoing analysis is found to afford an accurate picture of the transients upon disconnection, so long as the windings are well coupled, as is shown in Section III. Such coupling is best obtained by the use of parallel windings, wherein each turn of one coil is coupled to the same flux as the corresponding turn of the other coil. However, when the coils are wound concentrically, there is a departure from this ideal

TABLE VIII—CRITICAL-DAMPING MEASUREMENTS ON A WIRE SPRING (AG-55) RELAY

Observed Parameters at Critical Damping		Calculations						β_w	
$C(f)$	R_2'	$C_{eff} = C + C_d$	$(C_{eff})^{1/2}$	$R_s + R_2'$	G_s	$G_2 = G_s + G_e$	G_2/G_w	Experimental[†]	Theoretical (Fig. 4)
0.24×10^{-6}	0	0.24×10^{-6}		44.5	114,700	114,900	3.03	1.10	1.0
0.14	50	0.14		94.5	53,900	54,100	1.43	0.389	0.3
0.09	100	0.09		144.5	35,200	35,420	0.935	0.20	0.15
0.05	200	0.05		244.5	20,800	21,020	0.514	8.65×10^{-2}	5.5×10^{-2}
0.02	400	0.02		445	11,450	11,670	0.308	2.99	2.28
0.4×10^{-8}	1000	0.41×10^{-8}		1045	4,850	5,090	0.134	0.539	0.45
0.2	1500	0.217		1545	3,290	3,510	0.0925	0.27	0.22
0.103	2300	0.120		2345	2,170	2,390	0.0631	0.146	0.137
7.65×10^{-10}	2700	9.35×10^{-10}		2745	1,850	2,070	0.0546	0.112	0.106
4.55	3000	6.25	1.96×10^{-5}	3045	1,670	1,890	0.0499	7.46×10^{-4}	6.2×10^{-4}
2.15	3600	3.85	1.68	3645	1,392	1,612	0.0425	4.57	4.5
1.1	4400	2.8	1.49	4445	1,143	1,363	0.0360	3.2	3.3
0.52	5100	2.22	1.34	5145	988	1,208	0.0318	2.61	2.5
0.10	5800	1.80		5845	871	1,091	0.0288	2.11	2.0

Initial Data: $N_1 = 6525$ $R_w = 1125$
   $N_2 = 2260$ $R_s = 44.5$

   $G_w = N_1^2/R_w = 37.900$
   $G^2_{max} = N_2^2/R_s = 114,700$

Measured Value of $C_d = 170 \times 10^{-12}f$

* From these data, see Fig. 17, and infer that $G_e = 220$ mho, $\mathcal{P} = 2.6 \times 10^{-8}$ Wb/NI.
† $\beta_w = (CR_w^2/\mathcal{P}N_1^2)(1 + G_2/G_w) = 1.14 \times 10^6 (1 + G_2/G_w)C$.

situation due to independent transient currents which arise within the uncoupled portion of the main winding. An additional oscillatory condition develops in such cases, which is particularly noticeable for relays with copper sleeves, whose core losses tend to be very high; this condition becomes more and more noticeable when the circuit approaches critical damping or is well into the overdamped core-loss region. This behavior may be explained by recognizing the role of the uncoupled part of the primary winding, now to be discussed.

Recall that the core loss is governed by a term $G_2 \mathcal{P}/C$ representing the resistive losses in the secondary, and note that this term grows very large as C becomes small. Thus, in the critical damping region, this large term tends to block all flow of current in the primary inductance. However, that portion of the primary inductance which is not coupled to the secondary, i.e., which does not share the same common flux, will not experience opposition to current flow from the term $G_2 \mathcal{P}/C$ (because, for it, $G_2 = 0$). The uncoupled part of the winding provides a parallel path tending to bypass the main winding in series with its core-loss term, as shown by the dotted lines in Fig. 2b. Its inductance may be much less than that of the coupled part of the winding, but still capable of generating appreciable superimposed surges into the rest of the circuit. The equivalent circuit for this condition reverts to the simple case for which only coil losses apply (i.e., no secondary winding) but for which the inductance is represented by a new term

$$L'' = \mathcal{P}'' N_1^2 \tag{10}$$

where $\mathcal{P}''$ represents the effective differential permeance of that part of the coil which does not couple to the secondary. It may be found experimentally, or be approximated by rule of thumb, as discussed in Section III. The resulting oscillations, as to frequency, peak voltage, etc., may be predicted through the use of the equations in Table II, for the case that $G_2 = 0$, and using L'' to represent the inductance. Peak voltage effects for this case may be read from Fig. 8, where β is estimated by using $\mathcal{P}''$ for permeance. The oscillation frequency is approximated from the value of ω_o given in Table II:

$$f_0 = \frac{\omega_o}{2\pi} = \frac{1}{2\pi N_1 \sqrt{\mathcal{P}'' C}}. \tag{11}$$

Conversely, when the oscillation frequency is measured, corresponding to a given set of circuit conditions (i.e., β, G, etc.), the value of $\mathcal{P}''$ can be evaluated. Measurements on various relays are shown in Section

III to correlate well with this relation, where $\mathcal{O}''$ is found to have a value of about 0.6×10^{-8} Wb/NI for various structural types typical of telephone switching.

2.3 Determination of Peak Values of Contact Voltage, and Related Values of Charge and Current

The peak values of the time-dependent variables q_1 , i_1 , and V_c may be determined by differentiating the corresponding equations as given in Table IV with respect to t, setting the result equal to 0, solving for t under these conditions (designated t'), and then evaluating each of the original equations when t is replaced by t'. These steps together with the resulting expressions for t' and for q_1 , i_1 , or V_c are briefly outlined in Appendix B. The derivations apply to the previously noted general case which includes an RC network shunted across the load, but the resulting general expressions are too involved for a full treatment in the present report. When the network resistance R_n is set equal to zero, however, representing the simpler unprotected case, the resulting expressions are relatively convenient to work with. These expressions, which are also developed in Appendix B, are summarized in Table IX. The peak voltage relations hold greatest interest, and will now be considered in more detail.

As seen in Appendix B, and Table IX, the peak voltage expressions for an unprotected load ($R_n = 0$) are:

Condition	Time to Peak, t'	Contact Peak Voltage, V_p	
I	$t' = \dfrac{\pi - \varphi}{\omega}$	$V_p = V_o\left[1 + \beta_w^{-\frac{1}{2}} \exp\left(-\dfrac{\pi - \varphi}{\tan \theta}\right)\right]\cdot$	(12)
II	$= G_w\mathcal{O}\beta_w^{\frac{1}{2}}(1 + \beta_w^{\frac{1}{2}})^2$	$= V_o[1 + \beta_w^{-\frac{1}{2}}e^{-(1+\beta_w^{\frac{1}{2}})}]\,.$	(13)
III	$= -\dfrac{\varphi}{\omega}$	$= V_o\left[1 + \beta_w^{-\frac{1}{2}} \exp\left(-\dfrac{\varphi}{\tanh \theta}\right)\right]\cdot$	(14)

These equations express the peak voltage in terms of the variables β_w , θ, and φ. Actually, both θ and φ may also be expressed in terms of β_w and G_2/G_w (see Table III). The equations are given in the form shown for the sake of compactness. However, when computations are made, the more detailed values for these terms can be substituted from Table III. (The subscript w is used to indicate that the value of R in this case is only the winding resistance, i.e., $R_n = 0$).

For this case of unprotected load, equations (12), (13), and (14) may be used to plot the time-to-peak, and the peak voltage. It is

TABLE IX—PEAK-VOLTAGE AND RELATED EQUATIONS

| VARIABLE	GENERAL CASE t'	GENERAL CASE "PEAK" VALUE	WHEN $R_n=0$ t'	WHEN $R_n=0$ "PEAK" VALUE	WHEN $\left\{\begin{matrix}R_n=0\\G_2=0\end{matrix}\right.$ t'	WHEN $\left\{\begin{matrix}R_n=0\\G_2=0\end{matrix}\right.$ "PEAK" VALUE
CASE I — DOMINANT LOSSES						
q_{1MAX}	$\frac{\pi-\phi}{\omega}$	$K I_0 \frac{\sin\theta}{\omega_0 \sin\phi} e^{-\frac{\pi-\phi}{TAN\theta}}$	$\frac{\pi-\phi}{\omega}$	$CV_0\, \beta_w^{-1/2}\, e^{-\frac{\pi-\phi}{TAN\theta}}$	$\frac{\pi-\theta}{\omega}$	$CV_0\, \beta_w^{-1/2}\, e^{+\frac{TAN^{-1}\theta}{TAN\theta}}$
i_{1MIN}	$\frac{\pi+\theta-\phi}{\omega}$	$K I_0 \frac{\sin\theta}{\sin\phi} e^{-\frac{\pi+\theta-\phi}{TAN\theta}}$	$\frac{\pi+\theta-\phi}{\omega}$	$\frac{I_0}{\sqrt{1+G_2/G_w}}\, e^{-\frac{\pi+\theta-\phi}{TAN\theta}}$	$\frac{\pi}{\omega}$	$-I_0\, e^{-\frac{\pi}{TAN\theta}}$
v_{CMAX}	SEE APP. B	SEE APP. B	$\frac{\pi-\phi}{\omega}$	$V_0\left[1+\beta_w^{-1/2}\, e^{-\frac{\pi-\phi}{TAN\theta}}\right]$	$\frac{\pi-\theta}{\omega}$	$V_0\left[1+\beta_w^{-1/2}\, e^{-\frac{\pi}{TAN\theta}}\right]$
CASE II — CORE, $\frac{G_2\vartheta}{C} > R_w$						
q_1	$\frac{1}{b-a}$	$\frac{CV_0}{2}\left[\frac{KR'}{R_w}-2\right] e^{-\frac{b}{b-a}}$	$G_w\vartheta\,\beta_w^{1/2}(\beta_w^{1/2}+1)^2$	$CV_0\,\beta_w^{-1/2}\, e^{-(\beta_w^{1/2}+1)}$	THERE IS NO CORE-LOSS CRITICAL DAMPING FOR THIS CASE	
i_1	$\frac{2b-a}{b(b-a)}$	$-K I_0 \frac{(b-a)}{b}\, e^{-\frac{2b-a}{b-a}}$	$G_w\vartheta\,\beta_w^{1/2}(\beta_w^{1/2}+2)(\beta_w^{1/2}+1)$	$-\frac{I_0}{(\beta_w^{1/2}+1)}\, e^{-(\beta_w^{1/2}+2)}$		
v_c	SEE APP. B	SEE APP. B	$G_w\vartheta\,\beta_w^{1/2}(\beta_w^{1/2}+1)^2$	$V_0\left[1+\beta_w^{-1/2}\, e^{-(\beta_w^{1/2}+1)}\right]$		
$\left.\begin{matrix}q_1\\i_1\\v_c\end{matrix}\right\}$ — COIL, $\frac{G_2\vartheta}{C} < R_w$	THERE IS NO MAX. OR MIN.- ONLY A GRADUAL CHANGE TO FINAL VALUE		THERE IS NO MAX. OR MIN.- ONLY A GRADUAL CHANGE TO FINAL VALUE			
CASE III — CORE, $\frac{G_2\vartheta}{C} > R_w$						
q_1	$-\frac{\phi}{\omega}$	$K I_0 \frac{\sinh\theta}{\omega_0 \sinh\phi}\, e^{-\frac{\phi}{TANh\theta}}$	$-\frac{\phi}{\omega}$	$CV_0\,\beta_w^{-1/2}\, e^{-\frac{\phi}{TANh\theta}}$	THERE IS NO CORE-LOSS OVERDAMPED CONDITION FOR THIS CASE	
i_1	$\frac{\theta-\phi}{\omega}$	$K I_0 \frac{\sinh\theta}{\sinh\phi}\, e^{-\frac{\theta-\phi}{TANh\theta}}$	$\frac{\theta-\phi}{\omega}$	$\frac{I_0}{\sqrt{1+G_2/G_w}}\, e^{-\frac{\theta-\phi}{TANh\theta}}$		
v_c	SEE APP. B	SEE APP. B	$-\frac{\phi}{\omega}$	$V_0\left[1+\beta_w^{-1/2}\, e^{-\frac{\phi}{TANh\theta}}\right]$		
$\left.\begin{matrix}q_1\\i_1\\v_c\end{matrix}\right\}$ — COIL, $\frac{G_2\vartheta}{C} < R_w$	THERE IS NO MAX. OR MIN.- ONLY A GRADUAL CHANGE TO FINAL VALUE		THERE IS NO MAX. OR MIN.- ONLY A GRADUAL CHANGE TO FINAL VALUE			
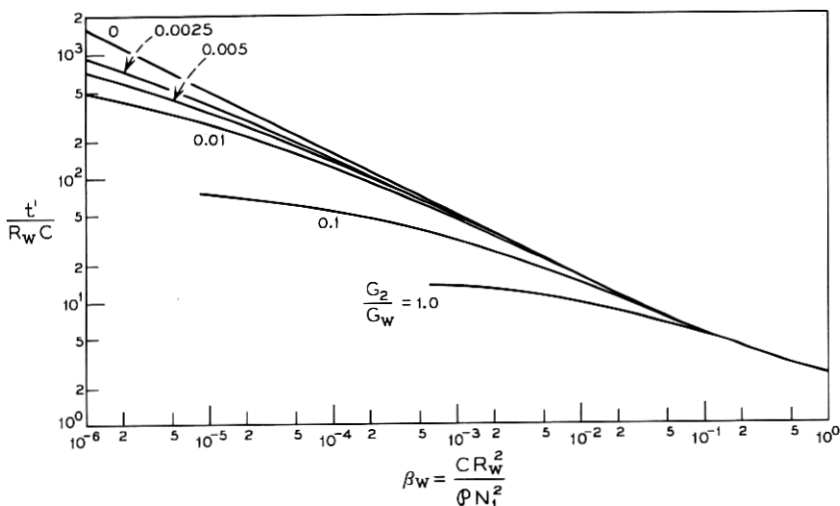
Fig. 6—Time, t', to reach peak voltage vs load design factor, β.

convenient to plot these in ratio form, using the ratio of peak time to capacitive time constant, t'/R_wC, and the ratio of peak voltage to battery voltage, V_p/V_o, respectively. These results are given in Figs. 6 and 7, as a function of β_w, for various values of G_2/G_w. They are found to be in good agreement with actual experience, as will be shown in Section 3.3, where measurements and theory are compared for both t' and V_p. It is seen that the ratio G_2/G_w has a pronounced influence
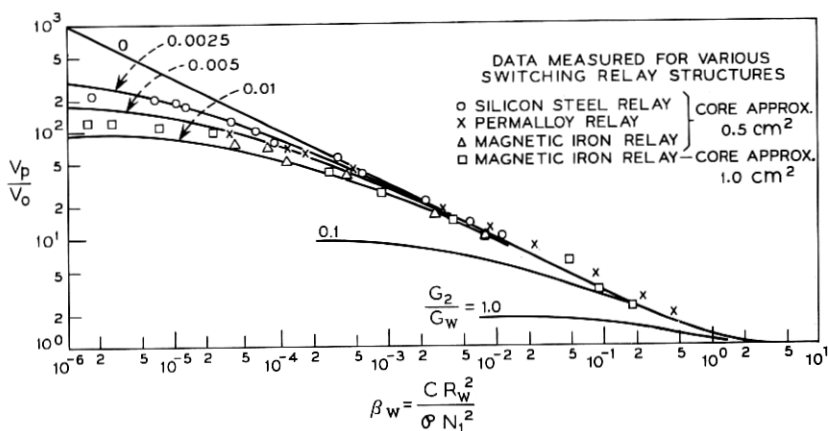

Fig. 7—Peak voltage, V_p, as a function of load design factor, β.

on the peak voltage across the opening contacts, and that even very small values of this ratio can lower the peak voltage and pulse time by several fold compared to the air core (i.e., nondissipative) case. This is particularly noticeable when small values of β_w (usually corresponding to small values of shunt capacitance) are involved.

A summary of the equations for the peak-related values of q_1, i_1, and V_c is also given in Table IX.

The relations determining these peak values may be used to restate the circuit equations in ratio form, if desired. As the contact voltage expressed in this form is of particular interest in later discussions, its value (when $R_n = 0$) is given below as

$$\frac{V_c - V_o}{V_p - V_o} = -\frac{\exp\left(-\frac{\pi - \varphi}{\tan \theta}(1 - \tau)\right)\sin\{(\pi - \varphi)\tau + \varphi + \theta\}}{\sin \theta}. \quad (15)$$

Equation (15) expresses the ratio of instantaneous to peak coil voltage as a function of the ratio of instantaneous to peak time, τ, following disconnection. A plot of this expression for two values of β_w is given in Fig. 8.

2.4. Energy Losses During the Surge

The surges just discussed can lead to breakdowns in wiring, in apparatus, or between the opening contacts. The breakdown itself is usually a very rapid event resulting from the discharge of the circuit capacitance through the low-impedance breakdown path of electrodes
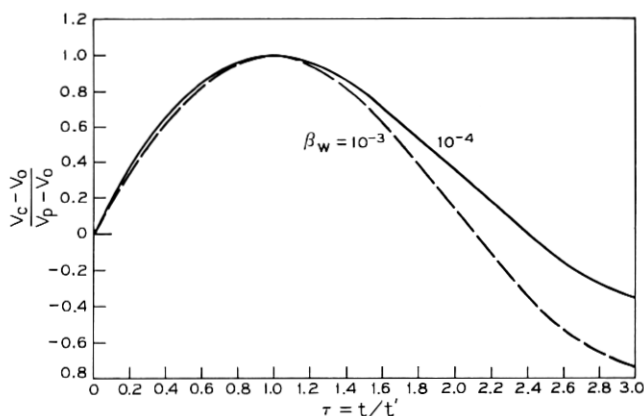

Fig. 8—Normalized plot of coil surge voltage ($V_c - V_o$) vs time.

and battery. The energy transferred from inductance to capacitance is thus the preponderant source of breakdown damage, and expressions are therefore needed to describe the manner in which the inductive energy is dissipated or transferred to the capacitor. In this section, a brief discussion is given of the breakdown process, followed by the derivation of energy expressions based on the foregoing circuit equations.

2.4.1 Breakdowns

The earlier expressions for contact voltage are of particular interest when breakdowns occur, because it is the value of voltage—matched against the dielectric strength of the wiring, of the connected apparatus, or of the contact itself—which determines when and how often breakdowns will occur. These breakdown possibilities are indicated in the simplified view of Fig. 9, which shows a typical voltage surge vs time after disconnection, and also two forms of dielectric characteristics representing the breakdown strength of portions of the circuit. The horizontal line, designated A, represents, for example, the breakdown characteristic of a pair of wires or apparatus terminals with constant spacing. The line of rising slope, designated B, represents the break-
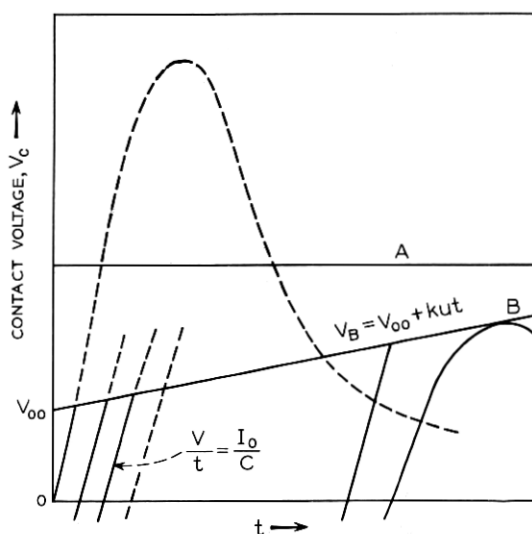

Fig. 9—Interaction between inductive surge and contact's dielectric characteristic (simplified view).

down characteristic of separating contacts. Its characteristic is well approximated by the equation

$$V_B = V_{oo} + kut \qquad (16)$$

(see for example Ref. 9)

where V_{oo} = minimum gas breakdown (usually the Paschen breakdown point which for air is about 320 volts),

k = slope constant (for air it is approximately 7×10^6 V/m), and

u = contact separation velocity.

There will be a gas breakdown whenever the coil's voltage characteristic, plus the battery voltage, exceeds the electrode separation characteristic, as is shown in the figure for the case of separating contacts. Each breakdown is commonly followed by an arc resulting from the discharge of the local capacitance, which was charged to a voltage $(V_B - V_o)$, through the low-impedance local wiring, usually causing a partial capacitive discharge and an extinction of the arc due to reverse oscillations. Following this, a new charging cycle begins which is similar to the earlier surge except rising toward a somewhat lower peak voltage representing the energy remaining in the load after the first breakdown. This procedure will continue repetitively until the residual load energy is insufficient to develop a surge whose peak value can reach the electrodes' dielectric breakdown.

For the constantly-spaced electrodes, each disconnection will lead to a group of multiple breakdowns which induce radiation in the wiring and a slow erosion of their surfaces. For example, fine-wire coils with too-close leadouts can eventually develop open-circuits as a result of this slow attrition.

Similarly, separating contacts experience an erosion of their surfaces. In the case of relay contacts, it is desirable to correlate the amount of erosion with the circuit parameters in order to determine either (i) the required contact volume to permit a given number of operations before failure, or (ii) the number of operations for a given contact volume. The remainder of this section will indicate one approach toward the correlation of contact erosion with the conditions of circuit and contact.

Many contact erosion studies have shown that the amount of metal lost is proportional to the energy dissipated between the electrodes during the discharge.[7,9] For the present case, a method of estimating this energy for the multiple breakdowns of the "B" type transient is therefore needed, and two alternate procedures are conceptually possible. The two approaches may be more clearly understood by a

reexamination of the oscilloscopic traces of coil current and contact voltage immediately following the contact opening, in Fig. 1. Each of the multiple surges for the mechanical contact is seen to be the early stage of an ideal contact surge which is interrupted when it reaches the breakdown characteristic of the contact gap, as is also indicated in Fig. 9. The breakdown is due to the voltage to which the capacitor is charged, plus the battery voltage, and when the breakdown does occur, it represents the discharge of this capacitance through the circuit comprising capacitance, contact, battery, and the low impedance of their wiring. This is a very rapid discharge, occurring in times that are negligible compared to the time required for the original surge to reach its breakdown value. The discharge is extinguished either by exhausting the capacitive stored energy $\frac{1}{2}C(V_B - V_o)^2$, or by reversals in voltage and current during the very high frequency breakdown discharge. Following extinction, a new surge develops as before. The energy dissipated in these multiple arcs may be approached in two ways: (i) by summing the individual energy terms (each of the form $\Delta E = \int_o^t V_A I_A \, dt$), where V_A is the characteristic voltage across the arc for the particular contact metal (typically about 14 volts) and I_A is the current through the arc, or (ii) by the total of the energy increments which are transferred from the coil to the capacitor to the arc (which should be related to the total initial inductive energy). Though the determination of V_A, I_A and t are subject to many difficulties of estimation, efforts to treat this problem with computer techniques have shown much promise.[10] The alternative procedure, namely to find the inductive energy which can be released into the arc, via the capacitor, will be considered here. Contact erosion should be strongly related to this energy, which will be discussed for the ideal inductive case in Section 2.4.2, and for the usual showering case in Section 2.4.3.

A more rigorous treatment must include the additional energy supplied from the battery during each breakdown arc, and an introductory discussion is given in Section 2.4.4.

2.4.2 *Energy Dissipation Following Disconnection—Ideal Contact*

First, let us find the energy consumed during the inductive surge, as a function of time. For simplicity, the analysis given here will consider the case that $R_n = 0$, i.e., the unprotected load. Based on the equivalent circuit of Fig. 2b, and equation (Ib) Col. 2 of Table IV, the energy dissipated in the circuit resistance is seen to be

$$E_{res} = \int_o^t i_1^2 R' \, dt = \frac{I_o^2 R'}{\sin^2 \varphi} \int_o^t e^{-2bt} \sin^2 (\omega t + \varphi) \, dt. \qquad (17)$$

Upon integrating between the limits indicated, this internally dissipated energy is found to be

$$E_{res} = \frac{L' I_o^2}{2 \sin^2 \varphi} [\{1 - \cos \theta \cos (2\varphi + \theta)\}$$
$$- e^{-2bt}\{1 - \cos \theta \cos [2(\omega t + \varphi) + \theta]\}]. \qquad (18)$$

A closer inspection of equation (18), and further rearrangement of terms based on the relations of Tables II and IV, gives the alternative expression

$$E_{res} = \frac{L_1 I_o^2}{2} (1 + G_2/G_w + \beta_w)$$
$$- e^{-2bt}\left[\frac{\sin^2 (\omega t + \varphi) + \sin^2 (\omega t + \varphi + \theta)}{\sin^2 \theta}\right] \qquad (19)$$

$$= E_o - E_u \qquad (20)$$

where E_o = initially available energy in coil and capacitance

$$= \tfrac{1}{2} L' I_o^2 + \tfrac{1}{2} C V_o^2, \qquad (21)$$

E_u = undissipated energy, i.e., that portion of initially stored energy, which, at time t, has not yet been dissipated

= E_{ind} , energy still stored in inductance, L',

+ E_{cap} , energy so far transferred to capacitor, C.

These expressions thus offer the means for quantitatively estimating the way in which the initially stored energy is either internally dissipated (in the resistive term R') or made available for release outside the system (i.e., stored in the capacitor).

The extent to which energy may be released outside the coil system, as for example into a contact arc, is perhaps more easily pictured by further reference to Fig. 2, recalling that, for the present discussion, $R_n = 0$. At the time when the capacitor C is charged to a value capable of producing a dielectric breakdown at a contact voltage, V_B , it possesses an energy content $\tfrac{1}{2} C (V_B - V_o)^2$ which can be rapidly dissipated in the low-impedance contact circuit during a breakdown. The maximum capacitive energy which can be so discharged occurs at the time t' and at the voltage V_p . t' is the time when the main circuit current

equals zero; at this instant all the undissipated inductive energy has been transferred into the capacitor. The energy in the system at this point, $E'_u = E_{cap}$, is therefore a useful measure of the maximum portion of the coil energy which can be released to do external damage. By substituting the value of t' from equation (12) into the second right-hand term of equation (19), this is seen to give

$$\frac{E_{cap}}{E_o}\bigg|_{max} = \frac{E'_u}{E_o} = \frac{\exp\left(-\dfrac{2(\pi - \varphi)}{\tan \theta}\right)}{1 + G_2/G_w + \beta_w}. \tag{22}$$

Equation (22) states the maximum fraction of the initial releasable inductive energy that would be capable of doing external damage. Since φ and θ are themselves (from Table III) expressible solely in terms of the circuit and relay design parameters β_w and G_2/G_w, this energy factor is similarly dependent on only these two variables. The result for a wide practical range of relay and circuit variables is given by the family of curves plotted in Fig. 10. It is interesting that these curves indicate a central range of values for β_w where the energy that can be externally released is a maximum, with lesser energy values for larger or smaller values of β_w. This seems physically reasonable because small values of β_w correspond to small values of C and rapid pulses, while large values of β_w correspond to slow pulses. Thus, for the short pulses, more energy is forced into eddy-current dissipation, while for the slow pulses there is ample time to dissipate energy in
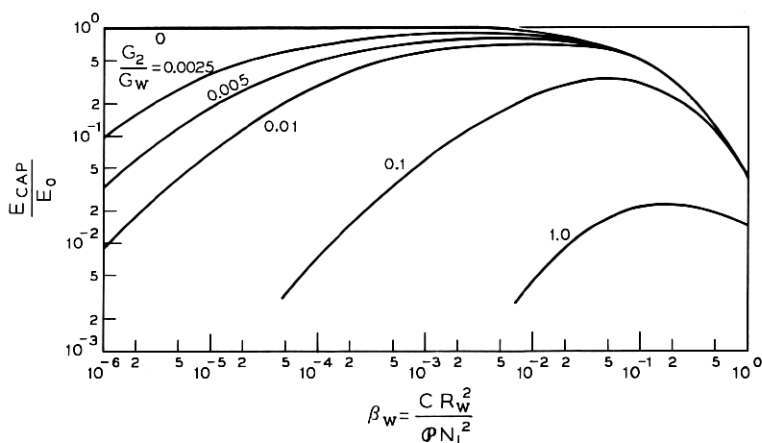
Fig. 10—Fraction of releasable energy, E_{cap}/E_o, available as potential source of arcing damage vs β.

the coil resistance before the capacitance is charged; for intermediate values of β_w, both dissipation terms are relatively small.

To summarize this concept of maximum releasable energy, consider an illustrative case for which the following circuit and relay design conditions are given:

Circuit: $V_o = 50$ volts, $C = 10^{-9}$ F, $I_o = 0.100$ ampere.

Relay Coil: $N_1 = 3100$ turns, $R_w = 500$ ohms,

$\mathcal{P} = 2.5 \times 10^{-8}$ Wb/NI, $G_2 = 100$ mho.

Determination of parameters and associated energy:

$$\beta_w = \frac{10^{-10} \times 250,000}{2.5 \times 10^{-8} \times 10^6} = 10^{-3}.$$

$$G_w = \frac{10^6}{500} = 20,000 \text{ mho}; \qquad G_2/G_w = 0.005.$$

$$E_o = \frac{2.5 \times 10^{-8}}{2} (3100 \times 0.1)^2$$

$$= 1.25 \times 10^{-3} \text{ J, initially available.}$$

From the chart: $E_{cap}/E_o = 0.74$, or maximum releasable energy $= 0.92 \times 10^{-3}$ joule. Since contact erosion is believed proportional to the energy delivered to the arc, this number is a useful starting point in establishing the system's erosion-inducing energy. For arcing contacts, it may be materially improved, it is believed, by an upward correction to the initial energy E_o as will be discussed in Section 2.4.4.

2.4.3 *Energy Dissipation During "B" Type Transient*

The preceding results are directly applicable to the repetitive breakdowns that occur between ordinary relay contacts that are separating in an air environment. The breakdowns occur when the surge voltage transient exceeds the dielectric breakdown characteristic of the contact gap, as previously discussed in Section 2.4.1 and illustrated in Fig. 9. Each breakdown occurs during a surge of the form of equation (15), which rises to intersect the contact characteristic given by equation (16) as illustrated in the figure.

2.4.3.1 *Steps During the Breakdown Process.* The energy losses during this series of breakdowns will thus be somewhat different from those in the idealized case discussed in Section 2.4.2 because they occur at an earlier stage of the surge. This effect may be visualized by considering the following simplified statement of representative sequential steps in the total breakdown process:

(*i*) The surge rises to a value of V_B given by equation (16). An amount of energy $\frac{1}{2}C(V_B - V_o)^2$ is released into the arc circuit while concurrently an amount of energy given by equation (19) is dissipated internally. The energy still remaining in the inductance to serve as a source for the next surge is E_{ind} and it comprises the initial energy of the previous surge minus the capacitive and resistive terms just mentioned. (A later and more rigorous study must also include the capacitive energy that is not dissipated during the surge, and so temporarily returned to the system, and also the energy replenishment from the battery.)

(*ii*) A new surge now develops which will rise toward a lower peak value defined by the inductive energy content after the previous surge, and a new breakdown occurs when a higher value of V_B is reached, as determined by the intersection of the coil surge with the contact's dielectric characteristic, equation (16). From the earlier work,[9] or from an inspection of Fig. 9, each new breakdown voltage is approximated by

$$V_{B_n} = V_{B_{n-1}}\left(1 + \frac{2kuC/I_o}{1 - 2kuc/I_o}\right) = V_{B_{n-1}}\left(\frac{1}{1 - 2kuC/I_o}\right) \quad (23)$$

These approximate expressions result from assuming (a) that the relevant part of the surge is closely represented by using its initial slope, i.e., $V/t = I_o/C$ when $t = 0$ (from Table V, Case I(d)), and (b) that the average initial current from the first to the last of the series of surges is given by $I_o/2$.

(*iii*) Similar steps continue until the amount of energy that must be imparted to the capacitor in order to produce a breakdown exceeds the energy remaining in the inductor. Further breakdowns cannot occur, and any remaining energy is dissipated in the coil's internal resistances.

2.4.3.2 *Energy Relations During the Surge.* An approximate method of estimating the energy that will be available as a driving source for arc damage will now be given. (One method would be to use a series of linear approximations for energy similar to that for V/t in item *ii* of Section 2.4.3.1. However, the procedure now to be given offers some simplicity, more rigor, and more insight into the mechanism of energy loss.) The method chosen requires a more detailed picture of the energy dissipation during the first stages of the surge, and a statement of the necessary energy content at each successively increasing breakdown voltage, now to be examined.

Equation (19) makes it possible to compare the energy lost in resistive elements, the energy still remaining in the inductor, and that stored in the capacitor, as a function of time. Thus, from equation (19),

$$\frac{E_{res}}{E_o} = 1 - \frac{E_{ind}}{E_o} - \frac{E_{cap}}{E_o}. \tag{24}$$

It is readily verified that the first and second $(\sin)^2$ terms in equation (19) define the inductive and capacitive energies, respectively. Normalizing these expressions, as was done for V_c in Section 2.3, we then write

$$\frac{E_{ind}}{E_o} = \frac{\exp\left(-\frac{2(\pi - \varphi)}{\tan \theta} \tau\right) \sin^2 \{(\pi - \varphi)\tau + \varphi\}}{(1 + G_2/G_w + \beta_w) \sin^2 \theta} \tag{25}$$

$$\frac{E_{cap}}{E_o} = \frac{\exp\left(-\frac{2(\pi - \varphi)}{\tan \theta} \tau\right) \sin^2 \{(\pi - \varphi)\tau + \varphi + \theta\}}{(1 + G_2/G_w + \beta_w) \sin^2 \theta}. \tag{26}$$

Equations (24), (25), and (26) are plotted in Fig. 11 for the case that $G_2/G_w = 0.005$, and two different values of β_w (= 10^{-4} and 10^{-3}). These curves show that the total losses during a discharge series may be divided between resistive and capacitive losses in quite different ratios, depending on the time at which the breakdown occurs, and also on the values of β_w and G_2/G_w. Thus, arc damage at the contacts, which comes only from the capacitive energy term, E_{cap}, will be a larger or a lesser fraction of the total initial inductive energy, depending
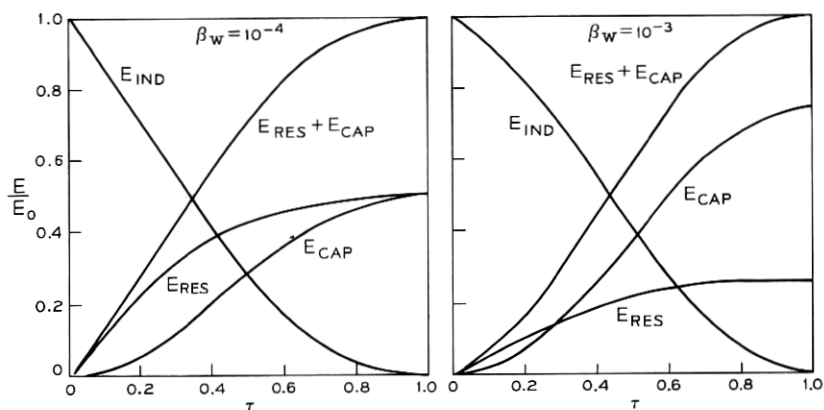

Fig. 11—Dynamic energy relationships during inductive surge. ($G_2/G_w = 0.005$).

on its ratio to the energy which is concurrently dissipated resistively, E_{res}. By means of the relations given here, these various forms of energy loss can now be calculated, based on the known properties of the control contact, the relay load, and the circuit between them. In illustration, it is evident from Fig. 11 that the resistive losses comprise a much higher fraction of the total initial energy for the lower value of $\beta_w(10^{-4})$. Accordingly, contact wear should be less for this case than for the case when $\beta_w = 10^{-3}$.

2.4.3.3 *Illustration.* The following example illustrates the steps for making a simple estimate of energy into the arc for a particular case. The needed starting data are as follows:

Given: ⎡ Control contact: separation velocity, u; V_B vs gap as given
⎢ by equation (16).
⎣ Circuit and load: R_w, N_1, C, G_2, V_o, NI_o, $\mathcal{P}$, $(R_n = 0)$.

Estimation of Energy:

(*i*) From above data, find $G_w = (N_1^2/R_w)$, G_2/G_w, and β_w.

(*ii*) Based on β_w and G_2/G_w, find V_p/V_o from Fig. 7, which in turn determines V_p.

(*iii*) The values of u, k, I, and C give a ratio which determines each successive new breakdown voltage according to equation (23). This in turn determines the capacitive energy which must be drawn from the inductive source, for each successive breakdown.

(*iv*) Reference to the normalized surge curves (Fig. 8) gives the normalized time for successive surge breakdowns, from which the values of E_{cap}, E_{res}, E_{ind}, and residual E_{ind} can be found (Fig. 11).

(*v*) This procedure is continued iteratively until the residual inductive energy is less than the required capacitive energy for the next sequential breakdown. At this point, no further breakdowns can occur. The cumulative capacitive energy ratio for all the breakdowns to this point then determines that portion of the initial energy which can produce contact arc damage.

These steps are of course conveniently performed by computer, but are not too complex for approximation using a slide rule. In one trial example: a relay with values of $G_2/G_w = 0.005$ and $\beta_w = 10^{-3}$, and other constants as in the example of Section 2.4.2, a slide-rule calculation indicated a series of 10 breakdowns, which checked with experiment, and gave at the time of the last breakdown:

$$\text{Cumulative} \quad \frac{E_{cap}}{E_o} = 0.34,$$

$$\text{Residual} \quad \frac{E_{ind}}{E_o} = 0.11,$$

$$\text{Cumulative} \quad \frac{E_{res}}{E_o} = 0.55.$$

Thus, the indicated energy which is capable of producing contact damage in this case was estimated to be

$$E_{cap} = 0.34 \times E_o$$
$$= 0.34 \times 1.25 \times 10^{-3}$$
$$= 0.425 \times 10^{-3} \quad \text{joule.}$$

In the specific example in Section 2.4.2, it had been estimated that the *maximum* releasable energy that could be expended in arcing was $0.74\ E_o$. However, in this extension of that case, where multiple breakdowns occur, with attendant changes in the ratio of resistive to capacitive losses, and with some energy still remaining in the system after the last breakdown, the energy releasable into the arc circuit is found to be only $0.34\ E_o$, i.e. about 46 percent of the hypothetical maximum. In general, it is expected that the energy releasable to cause arcing erosion will be considerably less than the maximum energy as given by Fig. 10, though roughly proportional to it.

As already discussed in Section 2.4.2, the above procedure ignores a replenishment of energy into the system, during each brief arcing interval, due to the closed-circuit paths for battery current into the capacitor and into the inductor. Correction for these effects, discussed in the next section, will modify the results just obtained; it is expected that an upward revision in E_o, which recognizes the circuit current as well as the initial inductive energy, will result. The stepwise analysis just given is therefore an approximate treatment. Its special value is the insight it offers into the apportionment of energy available at the onset of each surge between internal dissipative losses, and between capacitive and inductive portions, which are the potential sources for arcing and associated contact erosion.

2.4.4 *Modifications in Energy Term, E_o, Due to Replenishment of Inductive Energy During Showering Arcs*

When the capacitive energy is released into the arc, at breakdown, oscillations in the arc circuit tend to extinguish it before the full energy is released—either because contact voltage drops below the arc voltage or current falls below the minimum arc sustaining current. The unreleased energy remains in the system; some will be dissipated in the circuit resistance and some will be transferred to inductance and back

to capacitor, and so will contribute to later breakdowns. The total of such available energy has an upper limit already given by E_u' in equation (22), of the form

$$E_u' = E_o f(t)$$

where $E_o = \mathcal{P}(NI_o)^2/2$ and $\mathcal{P}$ represents the differential permeance at NI_o. But when additional energy is pumped back into the system, from the battery, during each arc, the term E_o must be replaced by $(E_o + E_i)$ where E_i is this incremental battery energy. Information about the term E_i is therefore essential to a full understanding of energy entering into the arcing and eroding process.

A first indication of the approximate values for E_i comes from empirical erosion studies such as those discussed in Ref. 9. In this work it was found that $E_i = kI_o$ where I_o is the steady state circuit current and k is a term related to (i) arc voltage (ii) total time of all the arcs, (iii) magnetic constants of the circuit, etc. For a particular group of telephone relays it has the approximate value $k = 0.1$ (in volt-seconds).

Further treatment of this correction term, which can be a major factor in some cases, is beyond the scope of the present paper. But because of its probable significance in many practical cases, its existence should be recognized. An extensive study of the importance of this battery-contributed energy replenishment, now nearly complete, by Pharney[11], confirms the importance of a corrective current term as indicated above.

III. EXPERIMENT

The foregoing analysis has been found to agree well with experiment for a variety of applications problems. Some of these experiments will now be summarized, indicating (i) experimental determinations for some of the important circuit constants, (ii) confirmation of various critical damping relations, and (iii) verification of the peak time and voltage relations. While the data apply specifically to the case of an unprotected load ($R_n = 0$), the methods seem equally applicable to future studies of the more complicated general case.

3.1 Evaluation of Circuit Parameters Which Describe the Relay Structure

The principal variables to be considered are the effective distributed capacitance of the coil, its effective inductance, and the core-loss term.

3.1.1 *Distributed Capacitance, C_d*

When one measures the voltage surges which develop upon disconnecting a coil in a circuit with very short wiring and no other apparent capacitance, it is found that the circuit behavior is as though a capacitance of the order of 50 to 200 pF were bridged across the coil. This is called the coil's effective distributed capacitance, C_d ; usually its value is fairly constant, for a particular basic structure and form of winding, regardless of number of turns, size wire, etc. This value should be known with fair accuracy in order to predict the relay's surge behavior in an actual circuit.

The initial slope of the surge voltage curve may be used to find this value of apparent capacitance for any particular coil structure. Note in Table V that, for the case that $R_n = 0$, the value of $\dot{V}_c$ at time $t = 0$, is

$$\frac{dV_c}{dt}\bigg|_o = \frac{I_o}{C}.$$

Thus, to estimate the value of C, one may open the coil circuit, preferably by means of an ideal contact, and note the initial slope of the voltage surge, which can be quite easily measured with an oscilloscope. Then the indicated value of shunt capacitance is

$$C = \frac{I_o}{\dot{V}_c}\bigg|_{t=o}. \tag{27}$$

This technique can be used to measure any given structure, when all external capacitance is carefully minimized. To avoid possible errors from use of a single measurement, it is sometimes worthwhile to repeat the above measurement after adding several different values of external shunt capacitance. Figure 12 demonstrates this procedure in a typical measurement made on a particular form of relay structure. The seven approximately straight lines on the oscillogram (Fig. 12a) are the initial slopes when the bridged capacitance was successively changed from 0 to 50, 100, 200, 400, 750, and 1000 pF. The upper trace is a measurement of current taken simultaneously, to give the proper value of I_o for substitution in equation (27). After making appropriate corrections for capacitance of the measuring leads, the apparent capacitance was calculated and plotted against the actual values used in the experiment. This plot is seen in Fig. 12b. The intercept on the apparent-capacitance scale corresponding to $C_{\text{external}} = 0$ is seen to be 140 pF, which is taken as the effective value of C_d for this particular test coil.
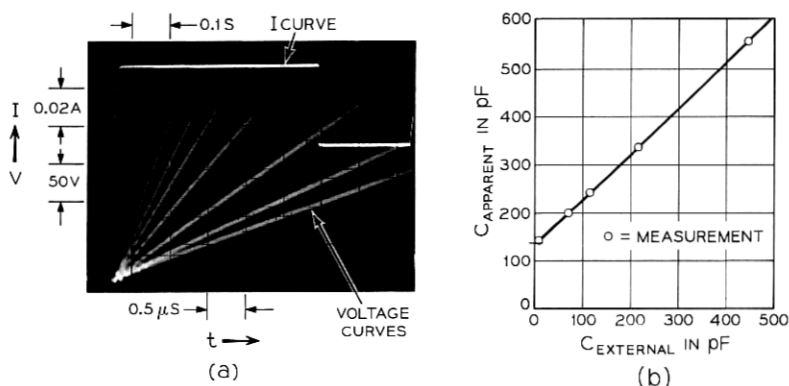
Fig. 12—Experimental determination of distributed capacitance, C_d. (a) Measurement of V_c and I_o. (b) Plot of C_{apparent} vs C_{external}.

Values for C_d which were measured for a number of different structural forms of relays are summarized below, together with brief data on relay construction.

Measured Values of C_d for Certain Relay Coils

Code Designa-tion	N_1	R_w	Relative Volume	Shape	Form of Structure	C_d
286	2,740	288	large	1/2 full	wire spring	120
280	26,550	12,450	large	full	polarized	125
AF33	11,850	950	medium	full	wire spring	140
AJ5	19,400	2,500	medium	full	wire spring	125
AJ7	34,900	9,100	medium	full	wire spring	110
AJ12	5,150	700	medium	short	wire spring	110
AJ57	P 3,235	200	medium	concentric	wire spring	140
	S 3,235	200	—	—	—	—
AJ503	2,110	270	medium	hollow	wire spring	200
AG55	P 6,525	1,000	medium	concentric	wire spring	180
	S 2,260	42	—	—	—	—
MA24	P 2,400	200	small	full	flat spring	115
	S 2,400	200	—	—	—	—
MB9	P 4,200	440	small	full	flat spring	170
	S 3,500	350	—	—	—	—
295A	5,180	525	medium	full	6 large mag. reed contacts	195
311A	3,950	550	small	full	3 small mag. reed contacts	210
327B	7,740	950	small	full	1 small mag. reed contact	140
327D	16,550	2,000	small	full	1 small mag. reed contact	150
Miniature Structure	4,300	1,560	very small	full	armature	80

3.1.2 *Effective Inductance*

The present study has postulated a circuit model which comprises lumped parameters, including the inductance. The inductance of an air core coil should rigorously satisfy this assumption. However, for coils using ferromagnetic materials, the flux linkages are a nonlinear function of the coil current. It is therefore necessary to consider the magnetization curve of the load circuit and to determine the effective working region for the particular load structure and circuit condition. This may be clarified by further considering the magnetization characteristic for a typical load structure shown in Fig. 3. The dotted curve shows a representative path that may have been followed by the prior operation of the unit, and point A indicates the starting condition of the inductive load at the time it is disconnected. The heavy curve is the demagnetization characteristic of the structure, which is the region of interest for the present discussion. Now, if the load is connected in a fast circuit (as for example with only a small capacitance) the circuit equations determine that the transient responses will be so fast that the core flux cannot change appreciably (being retarded by the core's eddy currents) in the time available during the early stages of the transient. In this case, the initial slope of the demagnetization curve (i.e., slope at Point A) should define the inductance quite accurately, and one may represent it as $L = \mathcal{P}N^2$ where $\mathcal{P}$ represents the differential permeance or slope of the demagnetization curve at the operated point, i.e.,

$$\mathcal{P}_o = \frac{d\Phi}{dNI}\bigg|_{I_o}.$$

However, if the load is in a slow circuit (for example with a large capacitance), there can be time for an appreciable amount of demagnetization. The inductance then grows larger as the transient progresses (i.e., $\mathcal{P}$ increases as the Φ-NI characteristic is traversed downward). The assumed lumped inductance no longer rigorously applies.

In the present study, for the sake of analytical simplicity, this variation will be either ignored, or be treated by assuming a progressively larger value of $\mathcal{P}$ as conditions combine to give slower transients. Based on the lumped-constant approach, $\mathcal{P}$ would be estimated by an averaging procedure over the portion of the demagnetization curve which is traversed during the transient. While it is believed that $\mathcal{P}_{av}$ will largely depend on the ratio of the peak transient time t'/RC to the core-loss transient time-constant, $G_2\mathcal{P}$, the subject is not treated

further here except as an averaged value of $\mathcal{P}$ is determined empirically. An averaged value of $\mathcal{P}$ is indicated in concept by the slope of dotted lines such as B in Fig. 3. Use of $\mathcal{P}_o$ usually gives good agreement with the analysis over several decades of variation in β.

$\mathcal{P}_o$ may be determined by magnetization data on the particular structure, or by various interpretations of actual surge measurements. While dynamic magnetization measurements are to be preferred, nevertheless static flux data have proven very useful. Determination using such a magnetic circuit approach is illustrated in Fig. 13. The two curves are actual demagnetization curves (taken statically) for two typical telephone relay structures: a standard wire-spring relay, and a flat-spring miniature relay. For the particular operated conditions shown, the resulting values of $\mathcal{P}_o$ are seen to be 1.8×10^{-8} Wb per ampere-turn in both cases. While these curves were obtained by measurements with a search coil, they could also have been estimated by well-known techniques of magnetic circuit analysis.

The effective inductance may be inferred based on measurements, in a known circuit, of the transient behavior of such properties as frequency, critical damping, peak voltage, initial slope, etc. A few of these are noted below.

3.1.2.1 *Frequency Method.* When circuit conditions are appropriate for an oscillatory response, as when $G_2\mathcal{P}/C$ and R_1 are approximately equal (discussed in Section 2.2), the frequency may be related to the circuit parameters based on relations given in Table II. Thus,
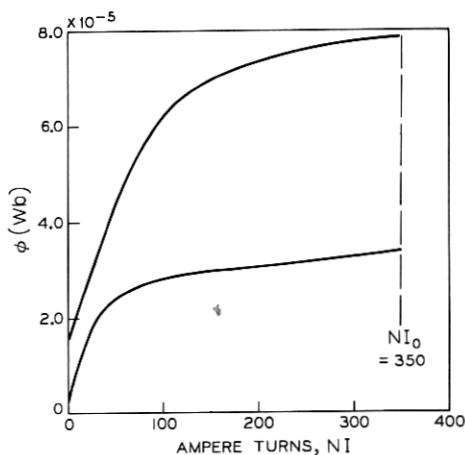

Fig. 13—Demagnetization curves of typical relays. Upper: AF relay. Lower: MA relay.

$$f = \frac{\omega_o}{2\pi} = \frac{1}{2\pi G_1 \mathcal{P} \sqrt{\beta_1(1 + G_2/G_1)}}$$

$$= \frac{1}{2\pi N_1 \sqrt{C\mathcal{P}(1 + G_2/G_1)}}$$

or

$$\mathcal{P} = \frac{1}{4\pi^2 N_1^2 Cf^2(1 + G_2/G_1)}. \tag{28}$$

Measured values of f, together with known values of N_1, G_1, and G_2 are substituted in equation (28) to find the effective value of $\mathcal{P}$.

3.1.2.2 *Method Based on Initial Slope of $\dot{V}_c$*. From Table V, note that when $t = 0$, $\dot{V}_c = 0$, for a load shunted by an RC network, when

$$CR_n^2 = L_1(1 + G_2/G_w)^2$$

or

$$\mathcal{P} = \frac{CR_n^2}{N_1^2(1 + G_2/G_w)^2} \tag{29}$$

Ordinarily, G_2/G_w is less than 0.01 and is neglected. Thus, in a circuit like Fig. 2a, one may vary R_n and C in various ways until oscilloscopic measurement of the contact voltage surge gives a zero initial slope. Because of its convenience, this method has been used extensively in the present study. It also provides some picture of how the inductance varies with the shunt capacitance which is a rough measure of the speed of the transient. The method is illustrated in Fig. 14. Figure 14a shows a family of surges for different values of R_n, with C fixed, and Fig. 14b shows a group of curves for which C and R_n have been adjusted to give $\dot{V}_c = 0$ at $t = 0$. The above procedure finds the combination of R_n and C for zero initial slope, and substitutes these values, together with N_1, into equation (29). The results for a variety of representative armature-type relay structures are summarized in Fig. 15. It is seen that varying the direct shunt capacitance C_s has a much larger influence on the variation of $\mathcal{P}$, than does varying C in the RC network, presumably because the pulse transient is so slowed that it encompasses a larger range of the demagnetization curve. The spread in the data for various structures is thought to be explained by the range of conditions for magnetic structure, stop disc height, operated ampere-turns, etc. Figure 16 gives a summary of the effective permeance for a wide range of sealed magnetic contact relays; the value of $\mathcal{P}$ is seen to be proportional to the number of contact units, as expected from magnetic
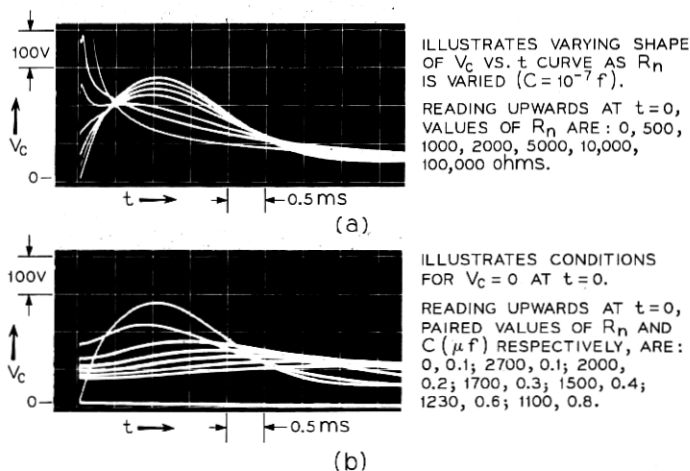
ILLUSTRATES VARYING SHAPE
OF V_c VS. t CURVE AS R_n
IS VARIED $(C = 10^{-7} f)$.

READING UPWARDS AT $t = 0$,
VALUES OF R_n ARE : 0, 500,
1000, 2000, 5000, 10,000,
100,000 ohms.

ILLUSTRATES CONDITIONS
FOR $V_c = 0$ AT $t = 0$.

READING UPWARDS AT $t = 0$,
PAIRED VALUES OF R_n AND
$C (\mu f)$ RESPECTIVELY, ARE :
0, 0.1; 2700, 0.1; 2000,
0.2; 1700, 0.3; 1500, 0.4;
1230, 0.6; 1100, 0.8.

Fig. 14—Illustration of method of measuring effective inductance, based on $\dot{V}_c = 0$ at $t = 0$. [AJ12 Relay; $N_1 = 5150$; R_w (hot) $= 877$ ohms.]

circuit analysis. Each contact adds a permeance of about 0.12×10^{-8} Wb/NI per unit. Departures from complete proportionality are attributed to different amounts of magnetic material in the return paths for various of these structures.

The above values are found to check well with values for $\mathcal{P}$ which are found as a by-product of other tests, as will be seen below.

One may estimate the initial effective stored inductive energy, which will be released into the system upon disconnection, by means of the relation

$$E_o = \tfrac{1}{2}\mathcal{P}(1 + G_2/G_w)(NI_o)^2 \qquad (30)$$

where NI_o is the value of ampere-turns at the point of release.

3.1.3 *Method of Determining Effective Eddy Current Conductance, G_e, of Relay Core*

The properties of a coupled secondary winding may be calculated directly from the relation $G_2 = N_2^2/R_2$ or from standard conductance formulas for copper sleeves.[4] When sleeves are used, their conductance values ordinarily outweigh the core's eddy current conductance to the point that it can be ignored. However, especially for unprotected applications, an estimate of the core's effective eddy current value is needed; and at the present time only experimental procedures seem suitable. Two such methods will now be discussed, one based on readings

of current or surge voltage at $t = 0$, and the other based on measurements of critical damping involving the use of a supplementary secondary winding.

3.1.3.1 *Method Based on Value of i_1 or V_e at $t = 0$.* An examination of the circuit variables indicates several equations where the term G_2/G_1 appears. For example, in Table V, the initial values of i_1 or V_e involve the term

$$K = \frac{1 + G_2/G_w}{1 + G_2/G_1} = \frac{i_1 \quad \text{at} \quad t = 0^+}{I_o}$$

$$= \frac{V_e \quad \text{at} \quad t = 0^+}{I_o R_n}.$$

Thus it is conceptually possible to measure G_2 by observing the value of K, experimentally, as by oscilloscope, for particular values of R_n and R_w. Rearrangement of the above expression then gives

$$G_2/G_w = \frac{1}{\dfrac{K}{1 - K} \dfrac{R_n}{R_w} - 1}. \tag{31}$$

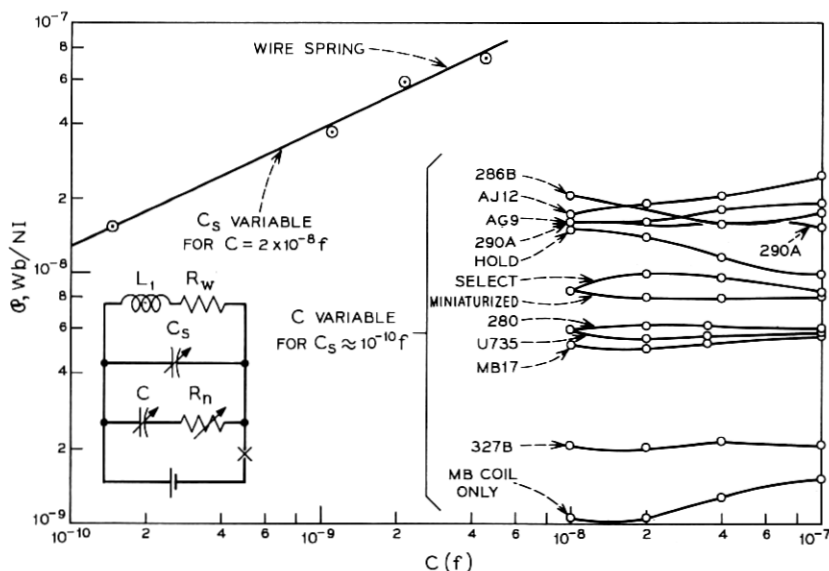However, for small values of G_2, the value of K will evidently be close

Fig. 15—Values of $\mathcal{P}$ determined by $\dot{V}_e = 0$ at $t = 0$ method (conventional relays).
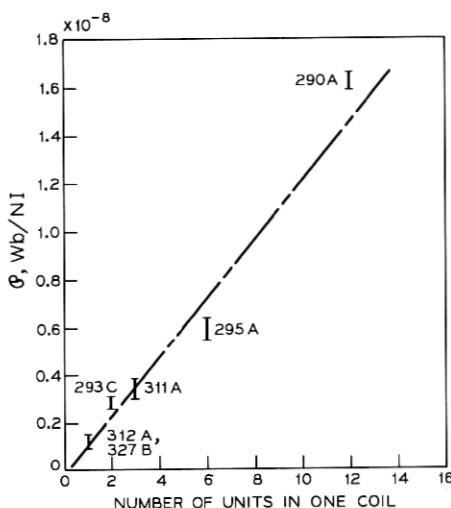
Fig. 16—Values of $\mathcal{P}$ determined by $\dot{V}_e = 0$ at $t = 0$ method (magnetic reed relays).

to unity, requiring experimental accuracies that seem quite difficult; therefore this method seems of doubtful value for measuring small values of G_2 , though probably useful when G_2/G_w exceeds about 0.1 as for copper sleeves, etc.

3.1.3.2 *Two-winding Method.* Instead, the method using two windings as already derived in Section 2.2.1 seems more useful. The procedure is to vary the shunt capacitance across the primary winding (with $R_n = 0$) and observe the value of series resistance across the secondary (or vice versa) for which critical damping is recognized on an oscilloscope. These steps are repeated over a range of values for C in the region of 10^{-10} to 10^{-9} F. After correcting C for the distributed capacitance of the primary winding, the resulting values of

$$ G_s = \frac{N_2^2}{R_2 + R_2'} $$

are plotted against $C^{\frac{1}{2}}$. In accordance with equation (9), the data tend to fall on a straight line whose zero intercept represents G_e . The effective permeance is then determined from the slope as

$$ \mathcal{P} = \frac{4N_1^2}{(\text{Slope})^2} . \tag{32} $$

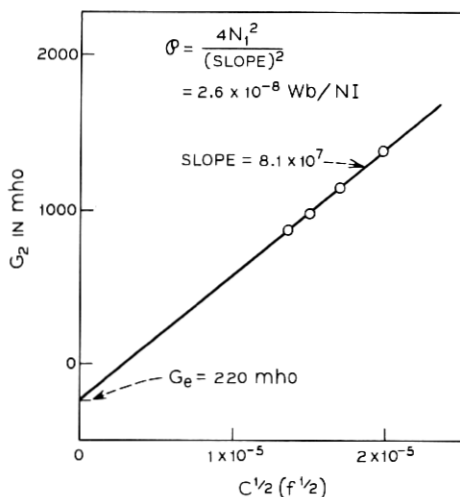Figure 17 illustrates this procedure for a typical wire spring relay.

Fig. 17—Experimental determination of eddy current conductance, G_e.

The data are from the small values for C and G_2, in Table VIII, which will be discussed in connection with more extended experiments on critical damping (Section 3.2). In the present experiment, the inferred value of G_e, which is the negative intercept on the G_2 axis of Fig. 17, is found to be 220 mho, and the slope is 0.81×10^8 mho $f^{-\frac{1}{2}}$, which from equation (32) gives $\mathcal{P} = 2.6 \times 10^{-8}$ Wb/NI.

3.2 Critical Damping Measurements

This section will describe measurements to verify the occurrence of critically damped relationships derived in Section 2.2, and to confirm the analysis for windings which are imperfectly coupled.

3.2.1 Critical-damping Boundaries

Determination of the effective eddy current term G_e described in the previous section is a by-product of an experiment to verify the analysis of Section 2.2 which derived relations for the boundaries between oscillatory and damped conditions. It was particularly interesting to verify the case for core losses dominant, as this relation had not previously been recognized. The procedure, as previously noted, was to interrupt the primary winding of a two-winding test coil with a mercury contact (to minimize arcing) and to observe the character of the interrupted surge as the values of G_2 and of the capacitance C across the primary were varied. (G_2 is varied by varying

the value of R_2' across its terminals). The value of the variable term for which the pulse changes from damped to oscillatory is fairly easy to recognize, using an oscilloscope. A set of such measurements is given in Table VIII together with calculations for plotting the data to check the validity of equation (5). The procedure was to (i) determine the corrected value of G_2 from equation (9), using the steps noted in the previous section and Fig. 17, (ii) tabulate G_2/G_w, and (iii) estimate the corresponding value of β_w.

A special consideration applies to this calculation of β_w. The analysis in Section II has shown that the effective inductance increases with G_2/G_w (see Table I) as follows:

$$L' = \mathcal{P}'(1 + G_2/G_w).$$

Here a prime has been added to the permeance term to indicate that $\mathcal{P}'$ represents the actual state of magnetization of the coil's magnetic circuit. The value of $\mathcal{P}$ in the formula $\beta_w = CR_w^2/\mathcal{P}N_1^2$ must be related to this experimental value as follows

$$\mathcal{P} = \mathcal{P}'/(1 + G_2/G_w).$$

Thus, for the present measurements, a correction has been applied so that β_w can be evaluated using the experimental value, $\mathcal{P}'$. The corrected value is

$$\beta_w = (CR_w^2/\mathcal{P}'N_1^2)(1 + G_2/G_w). \tag{33}$$

The values of β_w as estimated in this way, and as read from the curve, of Fig. 4, are listed in adjacent columns of Table VIII, and the experimental points are plotted as circles in Fig. 4. Agreement between experiment and analysis is seen to be good, especially considering that a constant value of $\mathcal{P}'$ has been assumed to apply over the whole range of the experiment.

The family of curves in Fig. 5 provides a convenient method for analyzing the data for a particular structure. In this case one plots the value of G_2/G_w vs the corrected shunt capacitance at critical damping. Then, based on the known values for N_1 and R_w for the given structure, one infers the effective value for $\mathcal{P}'$ from the numerical value for the appropriate curve, using the correction technique of the preceding paragraph. Data for several different structures with secondary windings are plotted, and also for several relays with copper sleeves. The copper sleeve cases are identified by a dot (measured value) surrounded by a rectangle representing the possible spread in the various parameters for a sample relay drawn from stock. The

copper sleeve relays represent the four standard sizes used in slow release relays for telephone switching. Agreement is again seen to be good.

3.2.2 Oscillations in Imperfectly Coupled Circuits

Measurements using secondary windings give somewhat different results depending on the form of winding used. When the primary and secondary are perfectly coupled, as with parallel-wound coils, the boundary between oscillatory and damped regions accords with the analysis given above. However, when primary and secondary are not perfectly coupled, as in the case of concentric windings, or of copper sleeves, a new and at first unexpected result is noted. In this case, there is a new form of oscillation which becomes noticeable as one operates near or beyond the region of critical damping—this is the discharge of the uncoupled portion of the inductance which is not attenuated by the core-loss term. The analytical basis was discussed in Section 2.2.2 and some data on numerical values will now be given.

The presence of shorted secondary windings which are not perfectly coupled to the primary winding was seen to lead to two superimposed transient patterns: (i) that due to the coupled portion of the winding which experiences critical damping below values of β determined by the coil losses, and (ii) that due to the uncoupled portion of the winding. For this group of windings, operating in the overdamped region, one observes oscillations in the circuit which are produced by the parallel inductive path of the uncoupled part of the main winding. Such oscillations are particularly noticeable with relays using copper sleeves. In fact the experimental observation of such oscillations is often helpful in the experimental determination of the critically-damped condition for the coupled portion of the winding. The following results are given as guides for dealing with these effects, which often need to be considered in the course of relay application studies. They are taken from extensive measurements on copper sleeve relays.

Among the general results were (i) the consistent observation that, when the coupled portion of the main winding was operating in the core-loss overdamped region, the amplitude and frequency of the oscillations for the uncoupled portion of the coil were independent of the value of G_2, and (ii) the frequency was proportional to $C^{-\frac{1}{2}}$, as predicted by equation (11). In addition, the critical damping boundary for four sizes of sleeve (covering a range of G_2 between about 40,000 and 200,000 mho) was measured. The data were then analyzed

to give the corrected value of effective core permeance for different values of G_2/G_1, in the same manner discussed in Section 3.2.1. This value of permeance $\mathcal{P}'$ is determined by using the value of β_w for a given value of G_2/G_w from the curves, Fig. 4, and substituting in equation (33), as is shown in the left-hand side of Table X. The spread in the indicated value of $\mathcal{P}'$ seems reasonable for a group of randomly selected stock relays.

The right-hand portion of the table shows measured values of frequency when the primary was shunted by a capacitor, $C = 10^{-8}$ F. Now, calling the effective value for this uncoupled inductance $L'' = \mathcal{P}''N_1^2$, all the test samples are seen to show values for $\mathcal{P}''$ of about 0.6×10^{-8} Wb/NI. This value can be used to estimate β, V_p, f, etc., for the uncoupled portion of the winding, for which $G_2 = 0$.

These data indicate that the uncoupled portion of the main winding can contain an appreciable energy which is externally releasable, even though the core-loss term due to the copper sleeve is very large. For example, for the relays studied in Table X, the initial releasable energy is about $E = 0.6 \times 10^{-8}(NI_o)^2$ joule.

The above concepts explain the general transient behavior of copper sleeve relays. The numerical values which are given for $\mathcal{P}$ only apply to the particular structural group of relays studied here (the slow-releasing class of the wire spring family).

3.3 Time-to-Peak, t', and Peak Voltage, V_p

Peak voltage measurements, i.e., measurement of the time-to-peak and the value of the peak voltage, offer further opportunities to check the analysis. The following discussion examines the measurements for both peak time and peak voltage on a single experimental unit, and also reconsiders a large series of peak voltage measurements which were made about 1953 based on then-current empirical practices.

3.3.1 Measurements of t' and V_p on a Sample Wire Spring Relay

The values of t' and V_p were measured on a test relay over a range of shunt capacitances, C, representing a large spread of the variable β_w. Based on the known constants of the structure, the formula for t'/R_wC, equation (12) as plotted on Fig. 7, and discussed in Section 2.3, was used to infer the associated value of β_w. This value of β_w was then used to predict the expected value of V_p/V_o, from Fig. 7. These results are summarized in Table XI, together with the measured values of V_p/V_o. The measured and predicted values for V_p/V_o are seen to agree very closely, and are taken to support the analysis.

TABLE X—COPPER SLEEVE RELAYS—MEASUREMENTS ON CRITICAL DAMPING AND UNCOUPLED INDUCTANCE

	Properties of Test Relay							Critical Damping Data			Uncoupled Inductance Data	
	Primary Coil				Secondary							
Code	N_1	R_w (ohms)	G_w (mho)	$[R_w/N_1]^2$	Sleeve*	G_2 (Nominal) (mho)	G_2/G_w	β_w (from Fig. 4)	C_{meas} for Crit. Damping (F)	θ' [From Eq. (32)] (Wb/NI)	f_{meas} for $C=10^{-8}$F (Hz)	θ'' [From Eq. (11)] (Wb/NI)
AG 10	10,050	996	100,000	0.00985	0.046″ Al	41,100	0.411	0.036	8×10^{-8}	3.1×10^{-8}	2040	0.61×10^{-8}
AG 13	16,050	2450	104,800	0.0231	0.046″ Cu	69,600	0.665	0.082	4.5×10^{-8}	2.1×10^{-8}	1330	0.56×10^{-8}
AG 15	7,800	702	86,700	0.0081	0.091″ Cu	130,200	1.503	0.33	4.8×10^{-7}	3.0×10^{-8}	2605	0.62×10^{-8}
AG 11	8,250	1180	57,700	0.0204	0.147″ Cu	194,700	3.37	1.15	4.5×10^{-7}	3.5×10^{-8}	2470	0.61×10^{-8}

* Wall Thickness, Material.

The final column in Table XI indicates the effective value of $\mathcal{P}$ for this same series of measurements. It is seen to have a fairly constant value for values of β_w greater than about 10^{-7}, and to gradually increase above this point. In line with earlier discussions, this increasing trend accords with the view that slower surges involve larger changes in the demagnetization curve and correspondingly larger values of $\mathcal{P}$. In keeping with this picture, it appears that the values of $\mathcal{P}$ as determined at the initial stages of the pulse (from $\dot{V}_c = 0$ at $t = 0$ in Section 3.1.2) should be increased by a factor of 2–3 when working with events at the peak of the pulse, where the flux curve has had more time to change.

3.3.2 Use of 1952 Data to Further Confirm Peak Voltage Relation

During a two-year period starting in about 1952, an extensive study was originated by M. M. Atalla, and later extended by many others, into the values for peak voltages when contacts open relay loads. The data were found to fit a formula relating V_p/V_o to a variable similar to the β_w term used in the present study, modified by an exponential term that was determined empirically. These very extensive data are available for comparison with the present analysis; their sources are unpublished Bell Laboratories memoranda. This earlier study used the following notation for the term designated β_w in the present work:

$$\beta_w = \mathcal{R}_o C \left(\frac{R}{N}\right)^2$$

where $\mathcal{R}_o$ represented the reluctance of the relay's magnetic circuit, and is the reciprocal of $\mathcal{P}$, the permeance as used in this report. This reluctance value, technically described as the "closed-gap reluctance," is a design constant which is tabulated for all telephone type relays. In the light of the present analysis, this value of reluctance, which represents the steepest slope of the *magnetization* curve, should be replaced by the uppermost slope of the *demagnetization* curve, representing a much higher reluctance (or lower permeance). Thus, all the earlier data can be used as a check on the present analysis if a relationship between these two figures is known. Data are not available for all the specific cases involved; however, it was determined from a review of magnetic data for many of these structures that a correction from the $\mathcal{R}_o$ values mentioned above to values for $\mathcal{R}$ which are related to the demagnetization curve could be approximated by increasing $\mathcal{R}_o$ by the factor 7.5. When this is done, when units are changed from

TABLE XI—MEASUREMENTS OF t' AND V_p

C (F)	$C + C_d$ (F)	Meas. t' (s)	$R_w C$	$t'/R_w C$	β_w (from Fig. 6)	V_p/V_o (from Fig. 7)	Meas. V_p/V_o	$C\left[\dfrac{R}{N}\right]^2$	Inferred $\mathcal{G}$ (Wb/NI)
0.825×10^{-9}	0.965×10^{-9}	34×10^{-9}	295×10^{-9}	115	1.5×10^{-4}	61	62	8.66×10^{-12}	5.77×10^{-8}
1.0	1.14	37	350	105	1.7	58	58	10.2	6.0
4.0	4.14	77.5	1.27×10^{-6}	61	6.0	36	37	37.0	6.16
0.01×10^{-6}	0.01×10^{-6}	128	306	41.9	1.3×10^{-3}	26	25	89.4	6.87
0.05	0.05	338	15.3	22.1	5.0	14	13	447	8.95
0.1	0.1	510	30.6	16.3	1×10^{-2}	10	10	894	8.94
0.5	0.5	1500	153	9.8	2.6	6.2	5.5	4470	17.2

Initial Data: $N_1 = 3235$ $R_w = 306$ (hot) $G_w = 34{,}200$ mho $(R/N)^2 = 0.00894$
$G_2 = 200$ mho (est.) $G_2/G_w = 0.0066$

Measured Value of $C_d = 140 \times 10^{-12}$ F

cgs to SI, and the new values of β_w are calculated, and $\mathcal{R}$ is converted to $\mathcal{P}$ (its reciprocal), a large number of data points for different structures becomes available for use here. The revised data points, taken from the unpublished memoranda, are plotted for various structures on Fig. 7. They are seen to show very good agreement between analysis and experiment for a wide range of telephone relays. The agreement could be further improved at the longer transient times (larger values of C or β_w) if an added correction for increasing differential permeance were made, along the lines indicated in Table XI (column showing "Inferred $\mathcal{P}$.")

Although the core-loss terms for these particular structures have not been measured by the methods outlined in this paper, the data points as plotted for the various structures in Fig. 7 are consistent with the expectation that large cores, or low-resistivity cores, should have larger values of G_2/G_w than small or high resistivity cores. These results therefore offer additional confirmation for the analysis of Section II.

SECTION IV. DISCUSSION

Based on the close agreement between analysis and experiment, the formulas given here appear well suited for use in analyzing the various transient effects associated with a contact opening an inductive load. Because of satisfactory prediction of pulse times, peak voltages, frequencies, and regions of damping or oscillation, it also seems reasonable to extend the use of these relations to the approximate estimation of energy dissipated in the contact arc, according to the analysis of Section 2.4.

Returning to the list of various problems discussed in Section I, the present study should therefore find application in the following areas.

(i) Prediction of surges from relay windings as a function of time, including breakdown values, times, oscillations, etc. The results apply equally to loads controlled by transistors, vacuum tubes, or relay contacts. While the examples are mainly given for the "unprotected" load, the basic formulas are available for the study of other cases.

(ii) Extension of the above work to predict the energy which will be internally dissipated or be made available via the capacitor to do damage in arcing, as in contact erosion. Extension of the present work is still needed to more fully evaluate the energy

replenished into the system from the battery during arcing. It is expected that continuing work[11] will improve understanding of the present empirical technique which relates contact erosion to the sum of an energy term and a current term.

(*iii*) Reasonable explanations now are available for earlier uncertain points.

(a) Relays with higher stop discs (i.e., larger operated air gaps) will ordinarily be less close to saturation. Therefore, their differential permeance will be larger than otherwise, which predicts a larger releasable stored energy. Although this configuration does not represent the condition for maximum total stored energy, (which must be at the smallest air gap), it does represent the condition for large *initial release* of magnetic energy, i.e., the value of $\mathcal{P}$ is larger.

(b) The oscillations which occur with copper sleeve relays are found to result from the uncoupled portion of the main winding. Relations are given for predicting their values.

(*iv*) Methods for predicting various behavior patterns are demonstrated.

(a) An example of a "B" type transient energy calculation is given.

(b) An extension of (a) above can be used to predict the final peak surge, following the last breakdown of a "B" type transient. Particularly with coils having a large number of turns, and a slowly rising surge, the number of breakdowns in a "B" type transient is relatively few. In such a case, a considerable residual inductive energy may remain following the last arc breakdown. The associated final surge tends toward higher than ordinary peak surges which need to be evaluated in order to insure adequate protection against breakdowns in the associated wiring.

(c) An analytical basis is available for determining the proper test conditions for coils being production-tested to withstand their own self-induced surge voltages.

(d) Many past evaluations of contact wear, and comparisons of various alloys and environments, are hard to compare with metals being studied today because the test conditions (magnetic structure of the load, circuit voltage, etc.) were so different from today's conditions. The relationships in this report are expected to permit the re-evaluation of some of this older data in a form that will permit comparisons on

a more universal basis. In one such test (1923), more than 250 metals and alloys in various gaseous environments were tested and compared. The review of this information in the context of today's applications problems should help to guide current design activities, as for example, those on sealed contacts.

(v) Future design for relay miniaturization can be better evaluated based on fuller understanding of the influence of the inductive load on the wear (and hence the necessary volume, travel allowance, and required work) of the contacts which control it. For example, the basic element determining contact wear is the effective *releasable* stored magnetic energy. The principal factor in this quantity is the initially stored effective energy term $\frac{1}{2}\mathcal{P}(NI_o)^2$, and often an additional term proportional to current I_o due to energy replenishment into the system by the battery, during arcing. Thus, contact erosion is related to the square of the operated ampere-turns and the differential permeance of the magnetic circuit's demagnetization curve, together with a term of approximate value $0.1\ I_o$. The most favorable condition is therefore that where the desired work output and operating time for the relay lead to a low value for NI_o (and also of current). The low value of NI_o is generally associated with a high-permeance magnetic circuit at the unoperated or critical gap condition. A high permeance at the closed-gap releasing current, however, is not compatible with low releasable energy. The present study suggests that contact life can be further improved if this sensitive unoperated structure were designed so that it is highly saturated (i.e., low $\mathcal{P}$) once it is in the operated position.

This releasable energy may be further reduced through the conscious use of a secondary winding whose value of G_2 is large enough to decrease the energy available for arcing by several fold while not being large enough to seriously influence release time. Typically, this means that one might profitably use a small closed secondary winding or copper sleeve having a value of G_2 equal to about 1000 to 5000 mho. If desired, the effect on operate time could be minimized by completing the secondary winding circuit through a diode which is poled to make the secondary effective only on release.

If, in this way, the load magnet can be made to cause less contact wear, the smaller contact wear allowance can result in a lowered mechanical work requirement. This in turn leads to a

smaller magnet structure, and so on. The concept should thus prove useful in design steps aiming to optimize a miniature relay structure, including the sealed magnetic reed types with their thin electroplated contact regions.

V. SUMMARY

This study has presented a group of analytical relations which describe the electrical transients when a contact opens an inductive load. In the past, relations based on a simple LRC analysis were found to be quite inaccurate. The present method expands the earlier approach to account for core losses, and is found to reduce to LRC-type relationships provided the lumped-constant terms have effective values as defined in Section II, and provided the value used for inductance recognizes the actual differential flux-ampere-turn characteristic for the particular load's magnetic circuit.

The analysis then leads to a group of useful relations for predicting surge times, peak voltages, or energies either consumed internally or available for external damage as in contact arcing. The analysis also predicts the conditions under which the surges are either oscillatory or damped. Experiments have confirmed these results, including the presence of two critically damped regions whenever the load possesses a finite secondary loss term. They have also explained the presence of an "anomalous" oscillatory condition for two-winding structures resulting from the uncoupled portion of the primary inductance.

Illustrations of how these results may be applied in circuit and relay design are given, as for example: the prediction of peak voltages, or of the chain of breakdowns in a "B" type transient; the estimation of energy available to produce contact erosion; and the determination of the oscillation frequencies in a given circuit. Experimental techniques were also described for determining the effective values of the various circuit constants, and typical values for a wide range of structures are given. The implications in relay design, as for miniaturization, are also discussed.

APPENDIX A

Derivation of Basic Circuit Equations for Current

The Disconnection of a Relay Winding-General Case (Assuming Ideal Break Contact, an RC Shunt Network, and a Secondary Winding)

Upon disconnection, transient currents will flow in the two meshes as shown in Fig. 2a. Using the notation of that figure, and of Table I,

the equations are

$$N_1 \frac{d\Phi}{dt} + i_1 R_1 + \frac{\int i_1 \, dt}{C} = 0 \\ N_2 \frac{d\Phi}{dt} + i_2 R_2 = 0 \Bigg\} . \tag{34}$$

These are interrelated through the magnetic circuit, for which we assume $\Phi = \Phi_1 + \Phi_2$, where Φ_1 and Φ_2 are proportional to the primary and secondary magnetizing forces, $N_1 i_1$ and $N_2 i_2$, respectively. Now designating $\mathcal{O}$ as the incremental permeance of the relay's magnetic circuit, i.e., $\mathcal{O} = d\varphi/dNi$, at the point in question, we write

$$\frac{d\Phi}{dt} = \mathcal{O} \left(\frac{dN_1 i_1}{dt} + \frac{dN_2 i_2}{dt} \right). \tag{35}$$

Making this substitution, the loop equations become

$$N_1 \mathcal{O} \left(\frac{dN_1 i_1}{dt} + \frac{dN_2 i_2}{dt} \right) + i_1 R_1 + \frac{\int i_1 \, dt}{C} = 0 \\ N_2 \mathcal{O} \left(\frac{dN_1 i_1}{dt} + \frac{dN_2 i_2}{dt} \right) + i_2 R_2 = 0 \Bigg\} . \tag{36}$$

We now adopt LaPlace Transform notation, and combine with initial conditions, which are that at $t = 0$, the charge on C is $(-V_o)$, and the core flux is $\Phi_o = \mathcal{O} N_1 I_o$. Equation (36) may then be rewritten:

$$N_1 \mathcal{O} s (N_1 i_1 + N_2 i_2) + i_1 R_1 + \frac{i_1}{sC} = N_1 \mathcal{O} N_1 I_o + \frac{V_o}{s} \\ N_2 \mathcal{O} s (N_1 i_1 + N_2 i_2) + i_2 R_2 = N_2 \mathcal{O} N_1 I_o \Bigg\} . \tag{37}$$

Using the second of these equations to find i_2, substituting into the first, and collecting terms:

$$i_1 = I_o \frac{N_1^2 \mathcal{O} (1 + G_2/G_w) s + R_w}{N_1^2 \mathcal{O} (1 + G_2/G_1) s^2 + \left(R_1 + \frac{G_2 \mathcal{O}}{C} \right) s + \frac{1}{C}}. \tag{38}$$

This is recognized as the expression for a simple R, L, C circuit, as shown in Fig. 2b, for which the inductance and resistance have *effective* values:

$$L' = L_1(1 + G_2/G_1) = N_1^2 \mathcal{P}(1 + G_2/G_1)$$

$$R' = R_1 + G_2\mathcal{P}/C.$$

Using these values, equation (38) becomes

$$i_1 = KI_o \frac{(s + a)}{(s + b)^2 + \omega^2} \tag{39}$$

where values of a, b, and ω are as given in Table II. Equation (39) is immediately solved by reference to tables of LaPlace Transforms. There are three cases:

$$\text{I. Oscillatory:} \qquad \omega_o^2 > b^2$$

$$\text{II. Critically Damped:} \qquad \omega_o^2 = b^2$$

$$\text{III. Overdamped:} \qquad \omega_o^2 < b^2$$

The solutions are found to be:

Case I.

$$i_1 = \frac{KI_o e^{-bt} \sin(\omega t + \varphi)}{\sin \varphi}$$

$$\text{where} \quad \varphi = \tan^{-1} \frac{\omega}{a - b}$$

Case II.

$$i_1 = KI_o e^{-bt}[1 + (a - b)t]$$

Case III.

$$i_1 = \frac{KI_o e^{-bt} \sinh(\omega t + \varphi)}{\sinh \varphi}$$

$$\text{where} \quad \varphi = \tanh^{-1} \frac{\omega}{a - b}$$

$$\tag{40}$$

(See Table III for more detailed summary of values for φ and related terms.)

APPENDIX B

Evaluation of Maximum or Minimum Values of q_1, i_1, and V_c

The procedure for these determinations is to differentiate the corresponding expression for q_1, i_1 or V_c given in Table IV, with respect

to t, and set the result equal to zero. This result, which defines the times at which the slope of the transient $= 0$, then determines either a maximum or a minimum condition, as will be shown. The first maximum or minimum will be designated t', i.e., "time-to-peak". The value for t' is then substituted into the original expression to give the "peak" value for q_1, i_1, or V_c (using the subscript p to designate it). While the analysis shows the steps taken for the general case of a shunt RC network, the resulting equations are often fairly cumbersome. Thus, after indicating the direction of these general results, they are fully expressed for the case of shunt capacitance alone ($R_n = 0$) which is the major subject of the present study. The steps are briefly outlined below:

Case I—Oscillatory (i.e., $\omega_o^2 > b^2$)

Charge

From Table IV, the time derivative of charge is

$$\frac{dq_1}{dt} = -\frac{Ki_o}{\omega_o \sin \varphi} \frac{d}{dt} [e^{-bt} \sin (\omega t + \theta + \varphi)]$$

$$= -\frac{Ki_o}{\omega_o \sin \varphi} e^{-bt} [\omega \cos (\omega t + \theta + \varphi) - b \sin (\omega t + \theta + \varphi)] = 0.$$

The derivative thus has a zero value when $t' = \infty$ or, based on phase angle relations indicated in Table III, when

$$\tan (\omega t' + \theta + \varphi) = \tan \theta,$$

which is only satisfied at values of t':

$$t'_q = \frac{\pi - \varphi}{\omega} , \qquad \frac{2\pi - \varphi}{\omega} , \qquad \text{etc.} \tag{41}$$

$$\text{(max)} \qquad \text{(min)} \qquad \text{etc.}$$

Substituting equation (41) into the original expression for q_1:

$$q_{1p} = +\frac{Ki_o}{\omega_o \sin \varphi} \sin \theta \exp \left(-\frac{\pi - \varphi}{\tan \theta} \right). \tag{42}$$

For the case when $R_n = 0$, from the relations in Tables II and III, this reduces to

$$q_{1p} = CV_o \beta_w^{-\frac{1}{2}} \exp \left(-\frac{\pi - \varphi}{\tan \theta} \right). \tag{43}$$

Current

From Table IV, the time derivative of current is

$$\frac{di_1}{dt} = \frac{Ki_o}{\sin \varphi} \frac{d}{dt} [e^{-bt} \sin (\omega t + \varphi)]$$

$$= \frac{Ki_o}{\sin \varphi} e^{-bt} [\omega \cos (\omega t + \varphi) - b \sin (\omega t + \varphi)].$$

The derivative thus has a zero value when $t' = \infty$ or, based on phase angle relations of Table III, when

$$\tan (\omega t' + \varphi) = \tan \theta,$$

which is only satisfied for values of t':

$$t_i' = \frac{\pi + \theta - \varphi}{\omega} , \qquad \frac{2\pi + \theta - \varphi}{\omega} , \qquad \text{etc.} \qquad (44)$$

$$\text{min*} \qquad , \qquad \text{max*} \qquad , \qquad \text{etc.}$$

Substituting equation (44) in the original expression for i_1 :

$$i_{1,p} = \frac{Ki_o \sin \theta}{\sin \varphi} \exp \left(-\frac{(\pi + \theta - \varphi)}{\tan \theta} \right). \qquad (45)$$

For the case when $R_n = 0$, from the relations in Fig. 4,

$$i_{1p} = \frac{i_o}{\sqrt{1 + G_2/G_w}} \exp \left(-\frac{(\pi + \theta - \varphi)}{\tan \theta} \right). \qquad (46)$$

Contact Voltage

From Table IV, the time derivative of contact voltage is

$$\frac{dV_c}{dt} = \frac{Ki_o}{\sin \varphi} \frac{d}{dt} \left[e^{-bt} \left\{ R_p \sin (\omega t + \varphi) - \frac{1}{\omega_o C} \sin (\omega t + \varphi - \theta) \right\} \right]$$

$$= \frac{Ki_o}{\sin \varphi} e^{-bt} \left[\frac{1}{C} \sin (\omega t + \varphi) - \omega_o R_p \sin (\omega t + \varphi - \theta) \right].$$

The derivative has a zero value when $t' = \infty$ or, based on phase angle relations of Table III, when

$$\tan (\omega t' + \varphi) = \frac{\tan \theta}{1 - \dfrac{1}{C\omega_o R_p \cos \theta}} ,$$

which is satisfied for values of t':

$$t_v' = \frac{1}{\omega} \left[\tan^{-1} \left\{ \frac{\tan \theta}{1 - \dfrac{1}{C\omega_o R_p \cos \theta}} \right\} - \varphi \right]. \qquad (47)$$

---

* (usually, however, there will be an initial maximum preceding min*, at $(\pi/2 - \varphi)$, when $\varphi < \pi/2$).

The general expression for peak voltage is then given by substituting equation (47) into the original voltage expression. The resulting rather complicated formula may be used to estimate peak voltages for the general case which includes an RC protection network, a procedure which is beyond the scope of the present report. For the case when $R_n = 0$, substituting values of the various terms from Tables II, III, and IV:

$$t' = \frac{\pi - \varphi}{\omega} \; , \qquad \frac{2\pi - \varphi}{\omega} \; , \quad \text{etc.}$$

$$\text{max} \; , \qquad \text{min} \; , \quad \text{etc.}$$

$$V_{cp} = V_o\left[1 + \beta_w^{-\frac{1}{2}} \exp\left(-\frac{\pi - \varphi}{\tan \theta}\right)\right]. \tag{48}$$

Case II—Critically Damped (i.e., $\omega_0^2 = b^2$)

For the critically damped case, as for Case I, the procedure is to find the time, t', at which zero slope of the time derivative of each variable occurs, and the corresponding "peak" value, for the general case which includes the RC network. Following this, the results are given for the specific case for $R_n = 0$, with individual consideration of the two critically-damped conditions: core losses dominant, and coil losses dominant.

Charge

From Table IV, the time derivative of charge is

$$\frac{dq_1}{dt} = -\frac{Ki_o}{b^2}\frac{d}{dt}\left[e^{-bt}\{a + b(a - b)t\}\right]$$

$$= -Ki_o e^{-bt}[(b - a)t - 1].$$

The derivative has a zero value when $t' = \infty$ or when

$$t'_q = \frac{1}{b - a}. \tag{49}$$

Substituting equation (49) into the original expression for q:

$$q_{1,p} = \frac{CV_o}{2}\left[\frac{KR'}{R_w} - 2\right]\exp\left(-\frac{b}{b - a}\right) \tag{50}$$

or

$$= 0.$$

Current

From Table IV, the time derivative of current is

$$\frac{di_1}{dt} = Ki_o \frac{d}{dt} [e^{-bt}\{1 + (a - b)t\}]$$

$$= -Ki_o e^{-bt}[b(b - a) - 2b + a].$$

The derivative has a zero value when $t_i' = \infty$, or when

$$t_i' = \frac{2b - a}{d(d - a)}. \tag{51}$$

Substituting equation (51) into the original expression for i_1 :

$$i_{1,p} = -Ki_o \frac{(b - a)}{b} \exp\left(-\frac{2b - a}{b - a}\right) \tag{52}$$

or

$$= 0.$$

Contact Voltage

From Table IV, the time derivative of the contact voltage is

$$\frac{dV_o}{dt} = -V_o \frac{d}{dt} \left[e^{-bt}\left\{1 - \frac{KR_n}{R_w} + (a - b)\left(\frac{b}{a} - \frac{KR_n}{R_w}\right)t\right\}\right]$$

$$= \frac{Ki_o}{C} e^{-bt}[1 - CR_n(2b - a) + (a - b)(1 - bCR_n)t].$$

The derivative has a zero value when $t_v' = \infty$, or when

$$t_v' = \frac{1 - CR_n(2b - a)}{(b - a)(1 - bCR_n)}. \tag{53}$$

and its value may be found by substituting equation (53) into the original voltage expression.

Cases Where $R_n = 0$

A more detailed treatment for the case where $R_n = 0$ will now be given, to indicate behavior under the two conditions for critical damping:

(*i*) Core losses dominant: i.e.,

$$\frac{G_2\mathcal{O}}{C} > R_w , \quad \text{or} \quad \frac{G_2}{G_1} < \beta_w , \quad \text{or} \quad b > a \quad (\beta_w > 0)$$

(*ii*) Coil losses dominant: i.e.,

$$R_w > \frac{G_2\mathcal{O}}{C} , \quad \text{or} \quad \beta_w < \frac{G_2}{G_1} , \quad \text{or} \quad a > b \quad (\beta_w \geq 4)$$

Then, the values of minimum or maximum circuit variable, and of corresponding times, are summarized below:

| (i) Core Losses Dominant | (ii) Coil Losses Dominant |

(i) Core Losses Dominant

Charge

$$t'_q = \frac{1}{b - a}$$

$$= G_w \mathcal{P} \beta_w^{\frac{1}{2}} (1 + \beta_w^{\frac{1}{2}})^2$$

$$q_{1p} = C V_o \beta_w^{-\frac{1}{2}} e^{-(1+\beta_w^{\frac{1}{2}})}$$

(ii) Coil Losses Dominant

$$t'_q = -\frac{1}{a - b}$$

As $a > b$, a negative, i.e., impossible, value of t' is indicated. Thus, $t'_q = \infty$ applies, and there is no peak value of q, which gradually decays to 0.

Current

$$t'_i = \frac{2b - a}{b(b - a)}$$

$$= G_w \mathcal{P} \beta_w^{\frac{1}{2}} (\beta_w^{\frac{1}{2}} + 2)(\beta_w^{\frac{1}{2}} + 1)$$

$$\dot{i}_{1,p} = -\frac{i_o}{(1 + \beta_w^{\frac{1}{2}})} e^{-(2+\beta_w^{\frac{1}{2}})}$$

$$t'_i = -\frac{2b - a}{b(a - b)}$$

As just above, this expression is always negative, and $t'_i = \infty$ applies, indicating no minimum, but a gradual decay to 0.

Contact Voltage

$$t'_v = \frac{1}{b - a}$$

$$= G_w \mathcal{P} \beta_w^{\frac{1}{2}} (1 + \beta_w^{\frac{1}{2}})^2$$

$$V_{cp} = V_o [1 + \beta_w^{-\frac{1}{2}} e^{-(1+\beta_w^{\frac{1}{2}})}]$$

$$t'_v = -\frac{1}{a - b}$$

As above, this expression is always negative, and $t'_v = \infty$ applies, indicating no maximum, but a gradual rise in contact voltage from 0 to V_o.

Case III—Overdamped (i.e., $b^2 > \omega_o^2$)

By following steps similar to those for Case I, except noting that the equations are in hyperbolic rather than trigonometric form, the conditions for maxima or minima are found to be as follows:

Charge

The condition for a maximum is that $t' = \infty$, or

$$\tanh (\omega t' + \theta + \varphi) = \tanh \theta.$$

The latter case is seen to be satisfied when

$$t'_q = -\frac{\varphi}{\omega}.\tag{54}$$

Now, recalling that $\varphi = \tanh^{-1} \omega/(a - b)$, it is seen that a positive (i.e., realistic) value of t' only occurs when $b > a$, which is the case where core losses are dominant. Therefore when coil losses are dominant, the charge gradually decays to zero.

The resulting peak value of charge, when $b > a$, is

$$q_{1p} = \frac{Ki_o \sinh \theta}{\omega_o \sinh \varphi} \exp\left(-\frac{\varphi}{\tanh \theta}\right)\tag{55}$$

where $\varphi = \tanh^{-1} \omega/(b - a)$.

For the case where $R_n = 0$, this reduces to

$$q_{1p} = CV_o\beta_w^{-\frac{1}{2}} \exp\left(-\frac{\varphi}{\tanh \theta}\right).\tag{56}$$

Current

The condition for a minimum is

$$\tanh(\omega t' + \varphi) = \tanh \theta$$

which is seen to be satisfied when $t' = \infty$, or when

$$t' = \frac{\theta - \varphi}{\omega}.$$

As φ is always greater than θ (see Table III), t' can only have a positive value when $b > a$, for which case

$$t' = \frac{\theta + \tanh^{-1} \dfrac{\omega}{b - a}}{\omega}.\tag{57}$$

There is no minimum for the case that $a > b$, except as the current gradually decays to zero.

The resulting peak value of current, when $b > a$, is

$$i_{1p} = \frac{KI_o \sinh \theta}{\sinh \varphi} \exp\left(-\frac{\theta - \varphi}{\tanh \theta}\right).\tag{58}$$

For the case where $R_n = 0$, this reduces to

$$i_{1p} = \frac{I_o}{\sqrt{1 + G_2/G_w}} \exp\left(-\frac{\theta - \varphi}{\tanh \theta}\right).\tag{59}$$

Contact Voltage

The condition for a maximum is that $t' = \infty$, or that

$$\tanh (\omega t' + \varphi) = \frac{\tanh \theta}{1 - \dfrac{1}{C\omega_o R_n \cosh \theta}}. \tag{60}$$

This expression may be used to give the peak voltage, when $b > a$, for the general case, as was indicated above for the oscillatory case.

For the case $R_n = 0$, the primary subject of the present paper, this becomes

$$\tanh (\omega t' + \varphi) = 0$$

or

$$t' = \frac{-\varphi}{\omega}. \tag{61}$$

As in the case of equation (54), this indicates a peak value of voltage only for the case where core loss dominates, for which

$$V_{cp} = V_o \left[1 + \beta_w^{-\frac{1}{4}} \exp \left(-\frac{\varphi}{\tanh \theta} \right) \right]. \tag{62}$$

When $a > b$, the voltage gradually rises to the asymptotic value $V_c = V_o$.

Summary

The foregoing expressions are summarized in Table VIII.

REFERENCES

1. Turney, T. H., "The Principles of Relay Timing in Connection With Automatic Telephone Circuits," J. IEE, *66*, No. 376 (April 1928), pp. 341–384.
2. Smith, Wagar, Vincent, and George, "Slow-Acting Relays," Electrical Engineering, *65*, December 1946, pp. 557–63.
3. Peek, R. L., Jr., "Principles of Slow Release Relay Design," B.S.T.J., *33*, No. 1 (January 1954), pp. 187–217.
4. Peek, R. L., Jr., and Wagar, H. N., *Switching Relay Design*, New York: Van Nostrand, 1955, Chapters 4 and 11.
5. Curtis, A. M., "Contact Phenomena in Telephone Switching Circuits," B.S.T.J., *19*, No. 1 (January 1940), pp. 40–62.
6. Atalla, M. M., "Discharge Phenomena on Break of Inductive Circuits," B.S.T.J., *33*, No. 3 (May 1954), pp. 535–558.
7. Germer, L. H., "Physical Processes in Contact Erosion," J. Appl., Phys. *29*, July 1958, pp. 1067–82.
8. Holm, R., *Electric Contacts*, Springer-Verlag, 1967, p. 313.
9. Wagar, H. N., "Predicting the Erosion of Switching Contacts That Break Inductive Loads," IEEE Trans. PMP, March 1969, pp. 16–24.
10. Mills, G. W., "The Mechanisms of the Showering Arc," IEEE Trans. PMP, March 1969, pp. 47–55.
11. Pharney, J. R., "A Closed Form Solution of the Arc Energy in a 'B' Type Transient Leading to a Simplified Prediction of Contact Life," to be published in Trans. Sixth Int. Conf. Electric Contact Phenomena, Chicago, Ill., June 5–8, 1972.